



**HAL**  
open science

## Evolution of a Holocene banner bank controlled by morphodynamics and structural setting of a macrotidal coast: Saint-Brieuc Bay (NW-Europe)

Kalil Traoré, David Menier, Erwan Gensac, Pascal Le Roy, Clément Lambert, Paul Bessin, Kevin Pedroja, Anne Duperret, Romain Le Gall

### ► To cite this version:

Kalil Traoré, David Menier, Erwan Gensac, Pascal Le Roy, Clément Lambert, et al.. Evolution of a Holocene banner bank controlled by morphodynamics and structural setting of a macrotidal coast: Saint-Brieuc Bay (NW-Europe). *Geoscience Frontiers*, 2021, 12 (5), pp.101183. 10.1016/j.gsf.2021.101183 . hal-03186763

**HAL Id: hal-03186763**

<https://hal.science/hal-03186763v1>

Submitted on 31 Mar 2021

**HAL** is a multi-disciplinary open access archive for the deposit and dissemination of scientific research documents, whether they are published or not. The documents may come from teaching and research institutions in France or abroad, or from public or private research centers.

L'archive ouverte pluridisciplinaire **HAL**, est destinée au dépôt et à la diffusion de documents scientifiques de niveau recherche, publiés ou non, émanant des établissements d'enseignement et de recherche français ou étrangers, des laboratoires publics ou privés.



Distributed under a Creative Commons Attribution - NoDerivatives 4.0 International License



## Research Paper

## Evolution of a Holocene banner bank controlled by morphodynamics and structural setting of a macrotidal coast: Saint-Brieuc Bay (NW-Europe)

Kalil Traoré <sup>a,\*</sup>, David Menier <sup>a</sup>, Erwan Gensac <sup>a</sup>, Pascal Le Roy <sup>b</sup>, Clément Lambert <sup>a</sup>, Paul Bessin <sup>c</sup>, Kevin Podoja <sup>d</sup>, Anne Duperret <sup>e</sup>, Romain Le Gall <sup>a</sup><sup>a</sup> Laboratoire Géoscience Océan, UMR 6538, CNRS, Université Bretagne Sud, Campus de Tohannic, 56000 Vannes, France<sup>b</sup> Laboratoire Géoscience Océan, UMR 6538, CNRS, IUEM, Université Bretagne Occidentale, 29280 Plouzané, France<sup>c</sup> Laboratoire de Planétologie et Géodynamique, UMR 6112, CNRS, Le Mans Université, Avenue Olivier Messiaen, 72085 Le Mans CEDEX 9, France<sup>d</sup> Laboratoire Morphodynamique Continentale et Côtière, UMR 6143, CNRS, Université Caen Normandie, campus 1, 2-4, Rue des Tilleuls, 14000 Caen cedex, France<sup>e</sup> Laboratoire Ondes et Milieux Complexes, UMR 6294, CNRS, Université Le Havre Normandie, 53 rue de Prony, CS, 80540, 76058 Le Havre cedex, France

## ARTICLE INFO

## Article history:

Received 18 December 2020

Received in revised form 23 February 2021

Accepted 27 February 2021

Available online 16 March 2021

Handling editor: M. Santosh

## Keywords:

Sand banks  
Banner bank  
Holocene climate  
Geomorphology  
Sea level rise  
Tidal gyre

## ABSTRACT

The morphology and internal structure of the Horaine Bank (Bay of Saint-Brieuc, NW France) are described based on multibeam echosounder and high-resolution seismic datasets coupled with vibro-core data. The Horaine Bank shows large-scale bedforms in the lee of a submerged rocky shoal, which allowed defining it as a Banner Bank. The internal structure of the sandbank reveals four seismic units (U1–U4) on a Cambrian basement (U0). The basal unit U1 is interpreted as reworked lowstand fluvial sediments those infilled micro incised valleys during a rise in sea level. This unit is overlain by paleo-coastal barrier sand-spit (U2) whose development was controlled by swell in the context of a rapid rise in sea level. The successive prograding unit (U3) is interpreted as flooding deposits in continuity with unit U2. The unit U4 is characterized by oblique reflectors oriented in two opposite directions. This last unit, dated post 3500 yr BP, corresponds to migrating dunes superimposed on the bank and observable in the high-resolution bathymetric data. The strong correlation between tidal currents and the apparent clockwise migration of dune crests suggests the presence of a tidal gyre controlling the present-day dynamics of most of the Horaine bank dunes. This study proposes a new model for the construction of banner banks characterized by the gradual transition of a sand spit to a banner bank during marine transgression and ensuing hydrodynamic variability.

© 2021 China University of Geosciences (Beijing) and Peking University. Production and hosting by Elsevier B.V. This is an open access article under the CC BY-NC-ND license (<http://creativecommons.org/licenses/by-nc-nd/4.0/>).

## 1. Introduction

Accumulations of Quaternary marine sedimentary deposits, which are associated with coastal prisms having low supply of sediments ('accommodation dominated shelves'; Swift and Thorne, 1991), occur in different forms and can be gathered into three categories: (i) systems tracts of deposits preserved within incised valleys (e.g., Lericolais et al., 2003; Menier et al., 2006; Sorrel et al., 2009; Chaumillon et al., 2010; Menier et al., 2010; Tessier et al., 2010, 2012; Gregoire et al., 2017; Wang et al., 2019) (ii) sandy veneers mostly of transgressive origin with no significant external morphology (e.g., Billeaud, 2007); (iii) shelf sediment bedforms whose building up is closely linked to hydrodynamic conditions (e.g., Reynaud, 1996; Franzetti et al., 2015; De Castro et al., 2017; De Castro and Lobo, 2018).

The Horaine Bank is a banner sandbank belonging to the third category. This type of sedimentary accumulation makes up composite and

complex bedforms, generally elongated, 10–50 m thick, up to 100 km long and >1 km wide (Reynaud, 1996; Snedden and Dalrymple, 1999). They are documented on open continental shelves, in estuaries and straits (Berné, 1999) at depths between 20 m and 50 m (Liu et al., 2007; De Castro et al., 2017) with the exception of certain banks such as in the Celtic Sea or in the Iroise Sea, which are located between depths of 80 m and 150 m (Reynaud, 1996; Marsset et al., 1999; Reynaud et al., 1999; Franzetti et al., 2015). These sediment bodies are interpreted as resulting from hydrodynamic phenomena (Huthnance, 1982; Hulscher et al., 1993). According to Berné et al. (1994), an initial irregularity of the bedrock is a necessary condition in the formation of these banks that can potentially generate an acceleration of currents on the flanks and result in the accretion of sediments in the central part of the bank. Depending on the hydrodynamic factors controlling their formation, these banks can be divided into two main families (Reynaud, 1996): (i) shoal retreat massifs: swell-dominated systems (the most frequently cited example is represented by the storm banks on the east coast of the USA described by Twichell (1984) in Reynaud (1996)) and, (ii) tidal bank systems in the southern North Sea

\* Corresponding author.

E-mail address: [kalil.traore@univ-ubs.fr](mailto:kalil.traore@univ-ubs.fr) (K. Traoré).

(Houbolt, 1968; Caston and Stride, 1970; Trentesaux et al., 1999) or in the Iroise Sea and the Western Channel (Walker, 2001; Franzetti et al., 2015).

The morphology of the Horaine Bank has already been the subject of summary mapping by Quesney (1983), complemented by a first morphological analysis of its internal structure (Augris et al., 1996). These previous authors describe a stack of seismic units such as observed in the Middelkerke bank in the North Sea (Berné et al., 1994), but do not specify the conditions and mode of formation. These composite systems are particularly interesting because they record changes in the depositional environment and variations in the balance between hydrodynamics and sedimentation during transgression-regression cycles. Furthermore, these sedimentary banks are an important source of marine aggregates and are, therefore, of major economic interest. An understanding of the mechanisms of their formation and evolution over time is necessary to define the conditions for sustainable exploitation of these resources.

However, few studies allow us to constrain the role of geological inheritance in the evolution of the build-up and dynamics of these

composite banks. Indeed, the Horaine Bank is developed behind submerged rocky coastal reefs, resulting from the structural heritage of the Bay of Saint-Brieuc, and is considered to have formed in a similar way as the tapering comet-tail shaped bedforms described by Guilcher (1950) in coastal areas. This comet-tail geometry implies specific sedimentary and hydrodynamic processes on the bank formation mechanisms and its present-day dynamics. In order to explore these points, we present multibeam echo sounder acoustic imagery, high-resolution seismic reflection (Sparker) and vibro-core drilling data (Fig. 1c), which are used to: (i) develop a detailed map of the morphological classes of the sedimentary bodies associated with the banner bank; (ii) specify the configuration of the internal structure of the bank using the stratigraphic approach described by Houbolt (1968) and Snedden and Dalrymple (1999); (iii) discuss the factors controlling the geographic location of the bank and highlight the role of sea-level variations in the sedimentary input and the bank architecture. Furthermore, we consider the genetic relationship between the offshore deposits and the nourishment of the adjacent coasts. We also investigate the sedimentary transit zone where the creation and migration of submarine

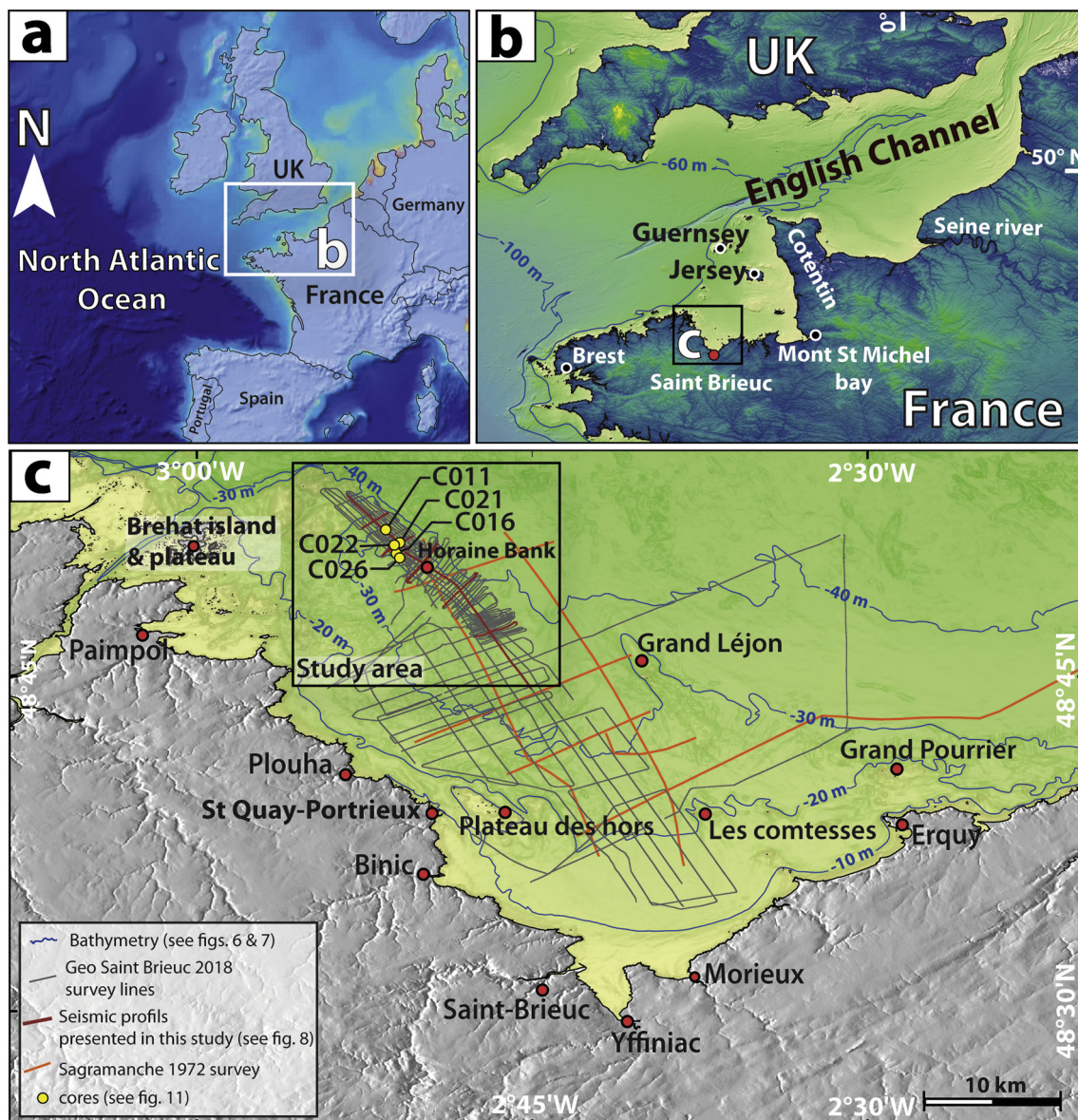


Fig. 1. Geographical location of the study area. (a) global location; (b) regional location; (c) Bay of Saint-Brieuc and location of the data used in this study.

dunes towards the coast can be observed. Finally, we propose a model of the present-day and long-term dynamics of the Horaine Bank to establish a framework for discussing its role in the sedimentary budget of the Bay of Saint-Brieuc.

## 2. Regional setting

### 2.1. Geology

The Bay of Saint-Brieuc is placed in the context of the North Armorican Domain, where the Palaeozoic basement is presently cropping out (Fig. 2). The North Armorican Domain contains the best-preserved remnants of the Cadomian orogen, characterized by major NE–SW ductile shear zones crossing the Bay of Saint-Brieuc and divided from NW to SE, encompassing three main units: the Trégor-La Hague, Saint-Brieuc and Saint Malo or Guingamp units, limited by the Locquemeau-Lézardrieux and La Fresnay shear zones, respectively (Chantraine et al., 2001; Ballèvre et al., 2013). The Trégor unit, which was very slightly deformed during the Cadomian orogenesis, is composed of a volcanic-plutonic complex, dated at 615 Ma (Graviou, 1992). The Saint-Brieuc unit is essentially made of a composite igneous suite affected by deformation and metamorphism corresponding to the inversion of the unit (Chantraine et al., 2001), in the time range between 620 Ma and 540 Ma, from Late Proterozoic to Early Cambrian (Auvray et al., 1980). The main Variscan deformation period started during the Devonian (420–360 Ma) and this orogeny constitutes one of the main inheritances in the continental crust in Brittany (Ballèvre et al., 2013). From the Carboniferous (345 Ma),

the formation of the Variscan cordillera is associated with the development of a set of major lithospheric-scale sub-vertical shear zones: the WNW–ESE North Armorican and South Armorican shear zones associated with secondary faults trending NW–SE, such as the Nort-sur-Erdre-Quessoy fault zone (Bitri et al., 2001). This NW–SE structure is assumed to have controlled the linear and transverse morphology of the western Saint-Brieuc Bay's coastline during its long-lived activity as early as the Triassic (Bois et al., 1991) and during the Eocene (Bonnet et al., 2000; Bessin, 2014).

### 2.2. Geomorphology

Bordering the Western Channel (Fig. 1), the Bay of Saint-Brieuc has a V-shaped coastline marked by numerous cliffs that can reach heights of >100 m. The bay extends over an area of approximately 800 km<sup>2</sup>, and forms a rocky platform sloping gently towards the open sea (0.1%) with a water depth not exceeding 40 m (Del Estal et al., 2019; Mathew et al., 2020). This coastal platform is characterized by the presence of numerous seabed features elongated and parallel to the two structural trends inherited from the Cadomian and Variscan orogenesis. These morphologic features correspond to either rocky shoals forming subtidal reefs such as the Plateau des Hors, or large sedimentary bedforms such as the Grand Léjon and Horaine banks.

To the northwest of the bay, the island of Bréhat rises from a wide rocky platform submerged to a water depth of 15 m (Fig. 3b). This rocky shoal extends from the mainland as far as 15 km offshore from the island, and its outer edge serves as a barrier behind which the

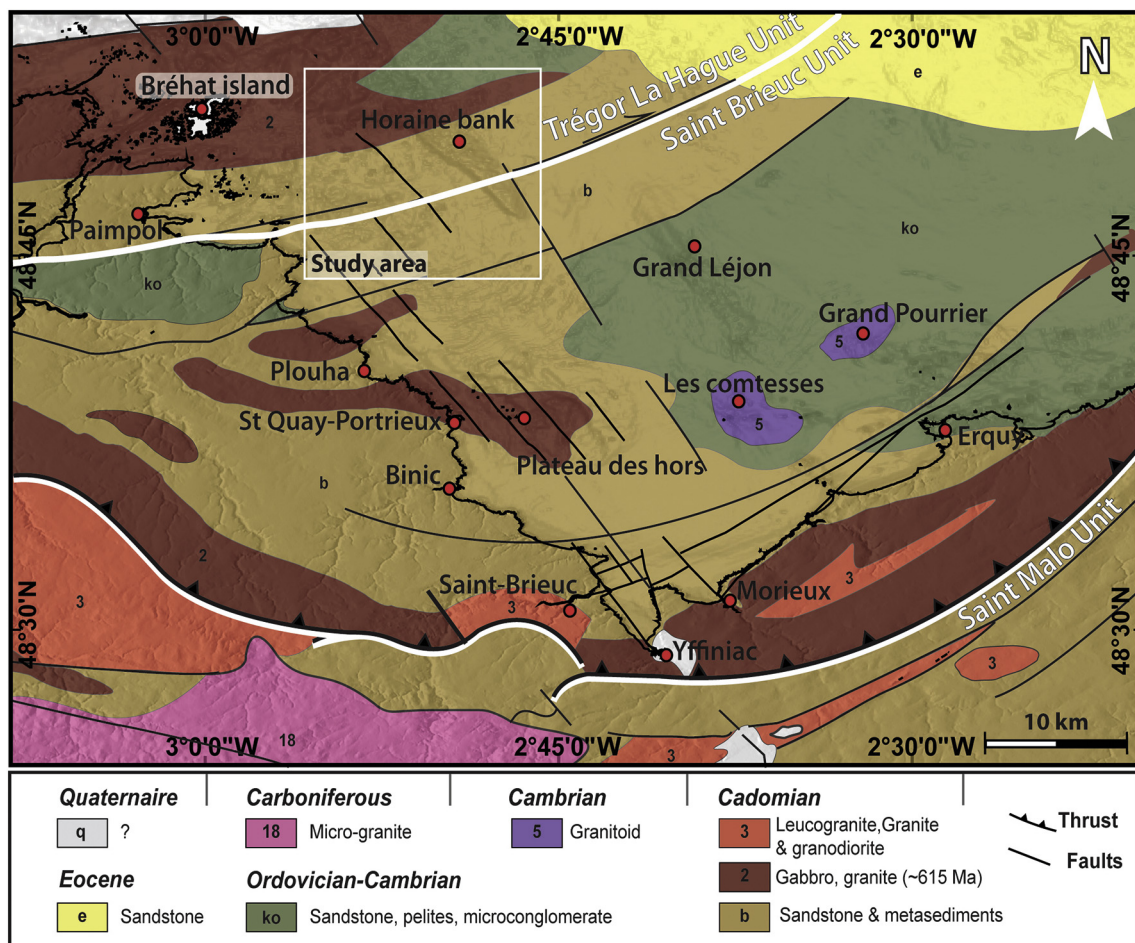
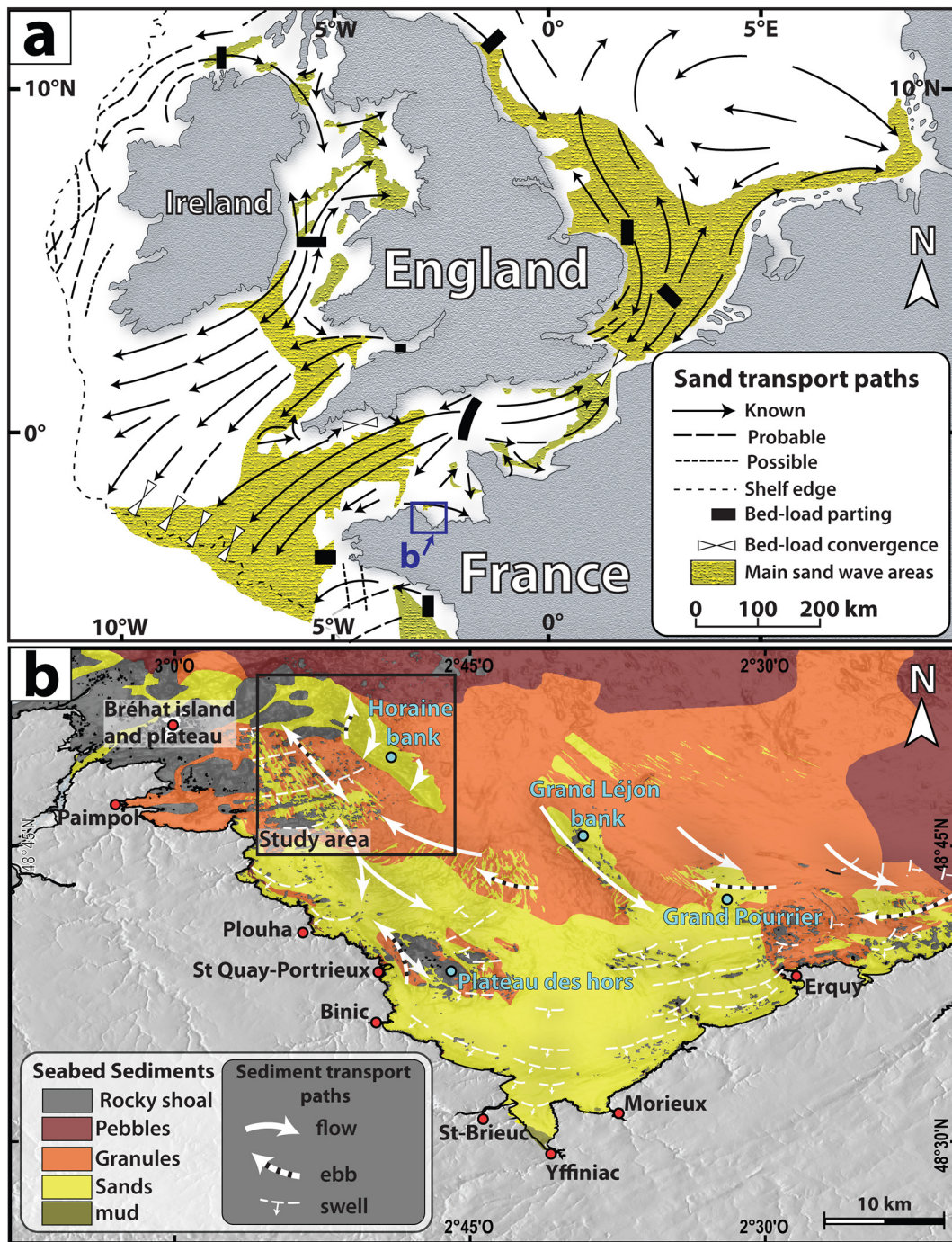


Fig. 2. Simplified geological map of the Bay of Saint-Brieuc (modified from Chantraine et al., 2003).



**Fig. 3.** Sedimentary context of the Bay of Saint-Brieuc. (a) Distribution of the dominant sand transport paths and their relationships with the main sand wave zones on the north-western European continental shelf (after Stride, 1963). (b) Map of surface sediments according to the Hydrographic and Oceanographic Service of the French Navy (S.H.O.M.), the arrows represent the hydrodynamic vectors of sedimentary transit in the Bay of Saint-Brieuc, identified from the types of bottom and sedimentary structures (after Augris et al., 1996).

Horaine banner bank was built. This limit probably reflects the more northerly position of the coastline when the sea level was 15 m lower about 8000 year BP (Lambeck, 1997; Stéphan and Goslin, 2014).

### 2.3. Oceanography

The Bay of Saint-Brieuc is subjected to semi-diurnal tides. The formation of a stationary tidal wave along the Cotentin peninsula (Fig. 4) gives rise to large tidal ranges along the south-western coasts of the English Channel (Larsonneur et al., 1994), reaching up to 12.3 m in the Bay of

Saint-Brieuc during the equinoctial spring tides (Fig. 4). The tidal currents associated with these large tidal range conditions, in particular near the Horaine Bank, can reach up to 4 knots ( $\sim 2 \text{ m}\cdot\text{s}^{-1}$ ) during flood tide and 3 knots ( $\sim 1.5 \text{ m}\cdot\text{s}^{-1}$ ) during ebb tide (Fig. 5) due to the channeling of currents, depending on the irregularities and incisions in the bedrock (Augris et al., 1996). The swell is mainly westerly and west-north-westerly, with its intensity fluctuating with the seasons and showing a maximum during the winter (mean  $H_s = 2 \text{ m}$ ; mean period = 10 s) with a minimum in summer (mean  $H_s = 1.5 \text{ m}$ ; mean period = 7 s) at the entrance to the Bay of Saint-Brieuc (Fig. 4, Bréhat

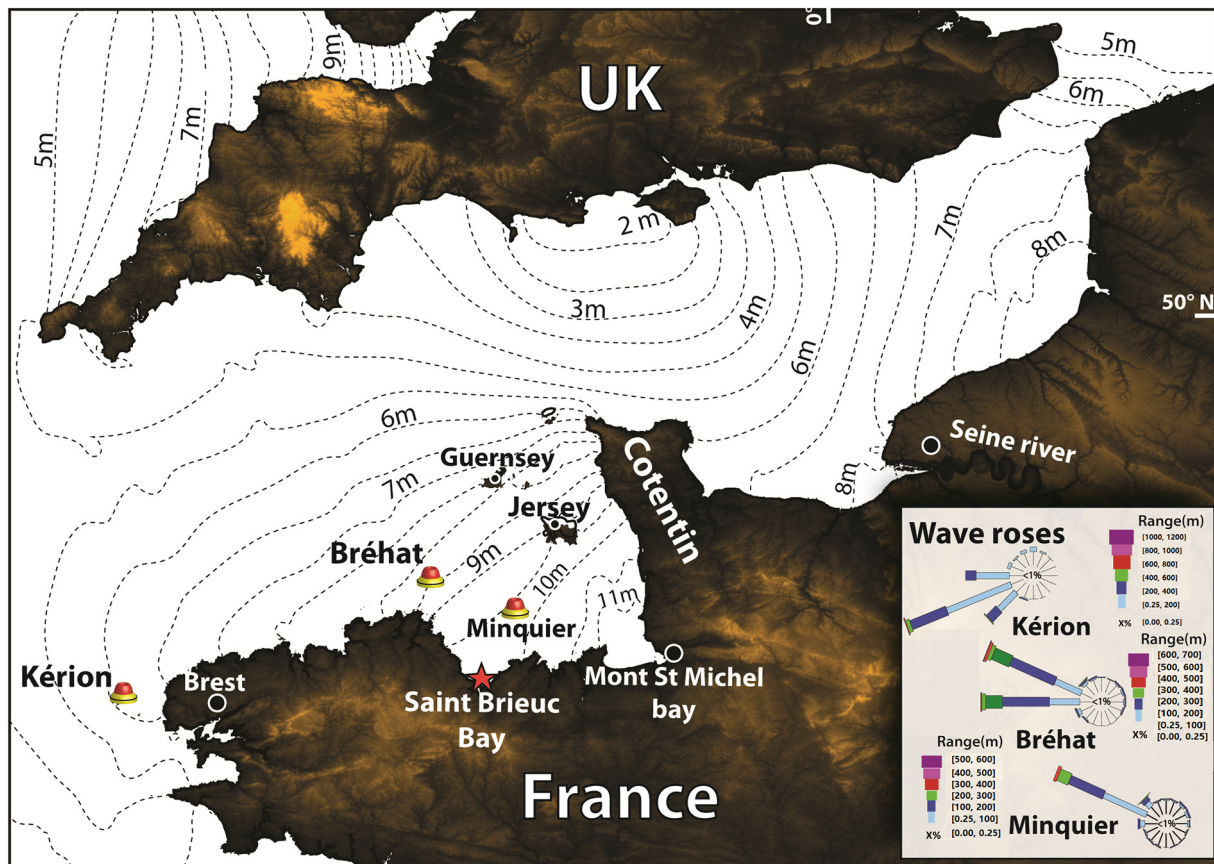


**Fig. 4.** Hydrodynamic context of the study area (Bay of Saint-Brieuc) located along the southwestern coast of the Channel, dominated mainly by the tide. The Black dashed lines represent the tidal amplitude data according to the *S.H.O.M* (1968); note the presence of swell coming from the Atlantic and recorded by the CANDHIS buoys represented on the map as Kérion, Bréhat and Minquier.

Buoy). However, the effect of swell waves on sediment dynamics is only slight compared to that of the tide (Augris et al., 1996).

### 3. Data and method

#### 3.1. Geophysical and sedimentological data acquisition

Our study is based on a combined analysis of bathymetric data, High Resolution (HR) to Very High Resolution (VHR) seismic reflection surveys and borehole data. We used new 600 km long VHR seismic lines (Sparker) and Multibeam EchoSounder (MBES) acoustic bathymetric acquisition, which were synchronously, acquired during the GeosaintBrieuc18 cruise (Menier, 2018) in order to obtain a corresponding bathymetry for each seismic line. The seismic and bathymetric profiles extend over the entire Bay of Saint-Brieuc (Fig. 1c) with a specific concentration of acquisition in the western part of the bay, more particularly, off the Island of Bréhat upon the Horaine Bank. The measured water depths range from 10 m to 35 m.

Due to the very low density of the acquisition in the eastern part of the bay, a complementary analysis of the seismic profiles was carried out by combining our new dataset with the SAGRAMANCHE1972 HR seismic cruise by IFREMER in 1972 that covers the eastern part of the bay (Fig. 1c). These complementary profiles allow us to carry out a comparative analysis of sedimentary thickness between the eastern and western parts of the Bay of Saint-Brieuc, and to replace the Horaine Bank in the sedimentary system of the bay.

In addition to bathymetric and VHR/HR seismic data, sedimentological data were acquired by sampling and coring during several cruises between 2018 and 2020. Based on the ca. 2.5 m long cores, 4 marker

horizons have been identified and dated through AMS radiocarbon dating on samples of shell sand that was carried out at the Poznań Radiocarbon Laboratory (Poland).

#### 3.2. Data processing and analysis

##### 3.2.1. Bathymetry

Processing of bathymetric data, which comprises geographical positioning, tidal correction and the relation to chart datum, was carried out using the Globe © (Global Oceanography and Bathymetry Explorer) Software V1.16.9 (Poncelet et al., 2020). The processing was completed by visual formatting using Fladermaus© and Adobe Illustrator CS5©. The bathymetric data were not interpolated to avoid any degradation of the morphological information of the sedimentary bodies.

The submarine dunes associated with the Horaine Bank were described according to their morphological parameters including height, orientation, crest depth and lee side angle. The determination of the morphometric parameters was carried out manually using ArcMap 10.2 © software from ESRI™ based on a method resulting from previous studies (Franzetti et al., 2013). 150 submarine dunes were listed on the Horaine Bank and classified in four classes according to a geostatistical analysis of their morphological characteristics.

##### 3.2.2. HR seismic data

The seismic data were processed using Unix seismic software. Wave filtration was carried out using the method described by Chaumillon et al. (2008). For the time-depth conversion, a seismic wave velocity of  $1700 \text{ m} \cdot \text{s}^{-1}$  was assumed for the infill sediments (Menier et al., 2010).

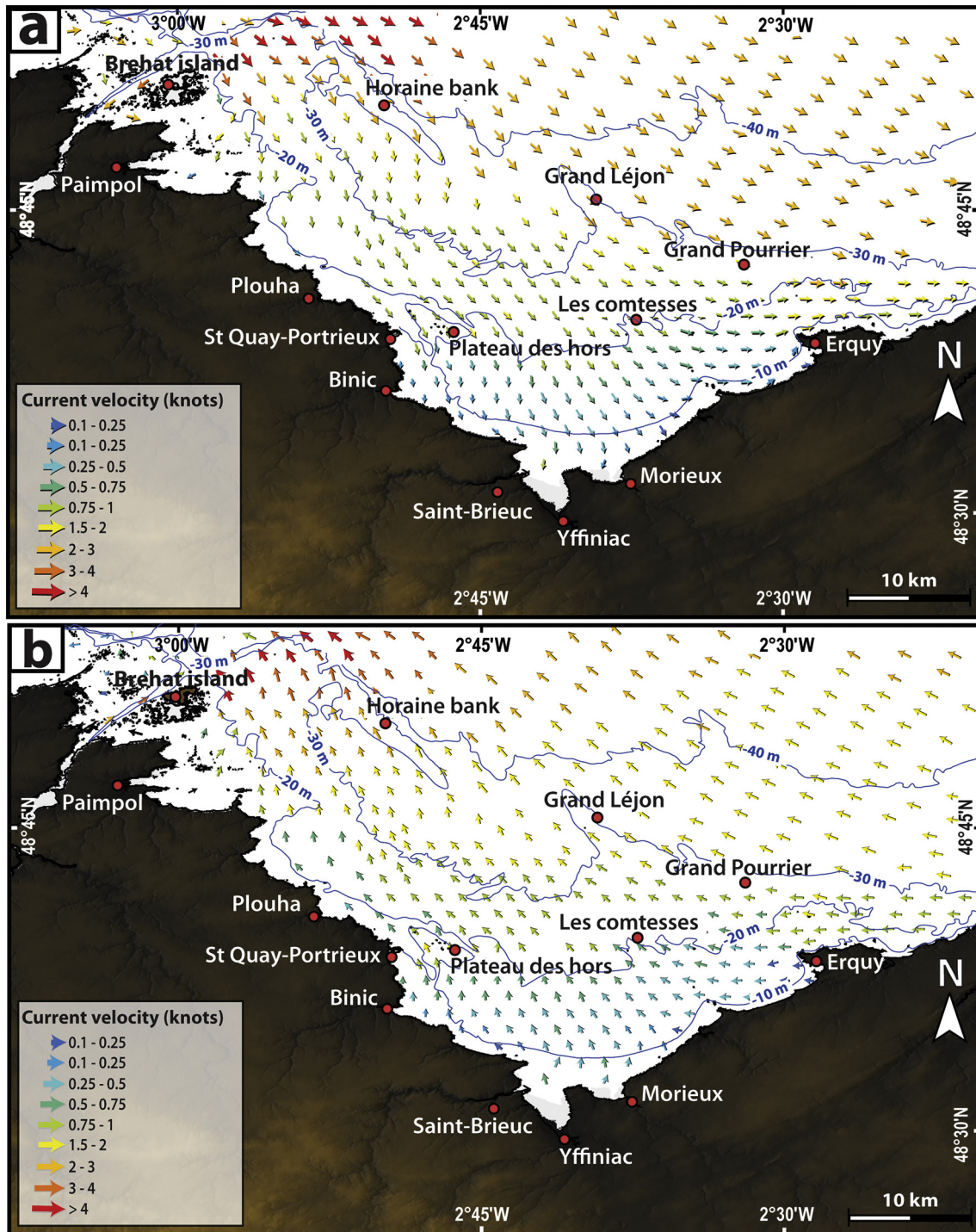


Fig. 5. Map of maximum surface tide currents in the Bay of Saint-Brieuc. Maximum velocities are reached at mid-tide (after S.H.O.M, 1968). (a) flow tide currents; (b) ebb tide currents.

### 3.2.3. Vibrocore data and radiocarbon dating

4 radiocarbon dates were acquired on shell sand (Table 3). All  $^{14}\text{C}$ -AMS dates were calibrated to calendar years with the CALIB 8.2 program using the Marine 20 calibration curve (Heaton et al., 2020) which considers a correction for the mean ocean surface reservoir age. The local deviation from the oceanic mean ( $\Delta R$ ) is estimated at  $-194 \pm 60$  years in the Bay of Saint-Brieuc (Tisnérat-Laborde et al., 2010). We applied this additional correction to all dating obtained on marine carbonate material. Thus, all the dates are expressed hereafter in calendar age (Cal.) BP ('before present', before 1950).

## 4. Results

### 4.1. External structure

The Horaine Bank shows an elongated banner morphology trending NW–SE in the lee of a high rocky shoal. It is 12 km long, 2 km wide and about 25 m thick and its depth is between 33 m and 9 m. A N–S trending crest shapes the top of the bank (Fig. 6). The Bank is asymmetrical, westward shifted with respect to the axis of the bank. It forms a steeper western flank with a slope of ca.  $5^\circ$  and a southeastern flank with a

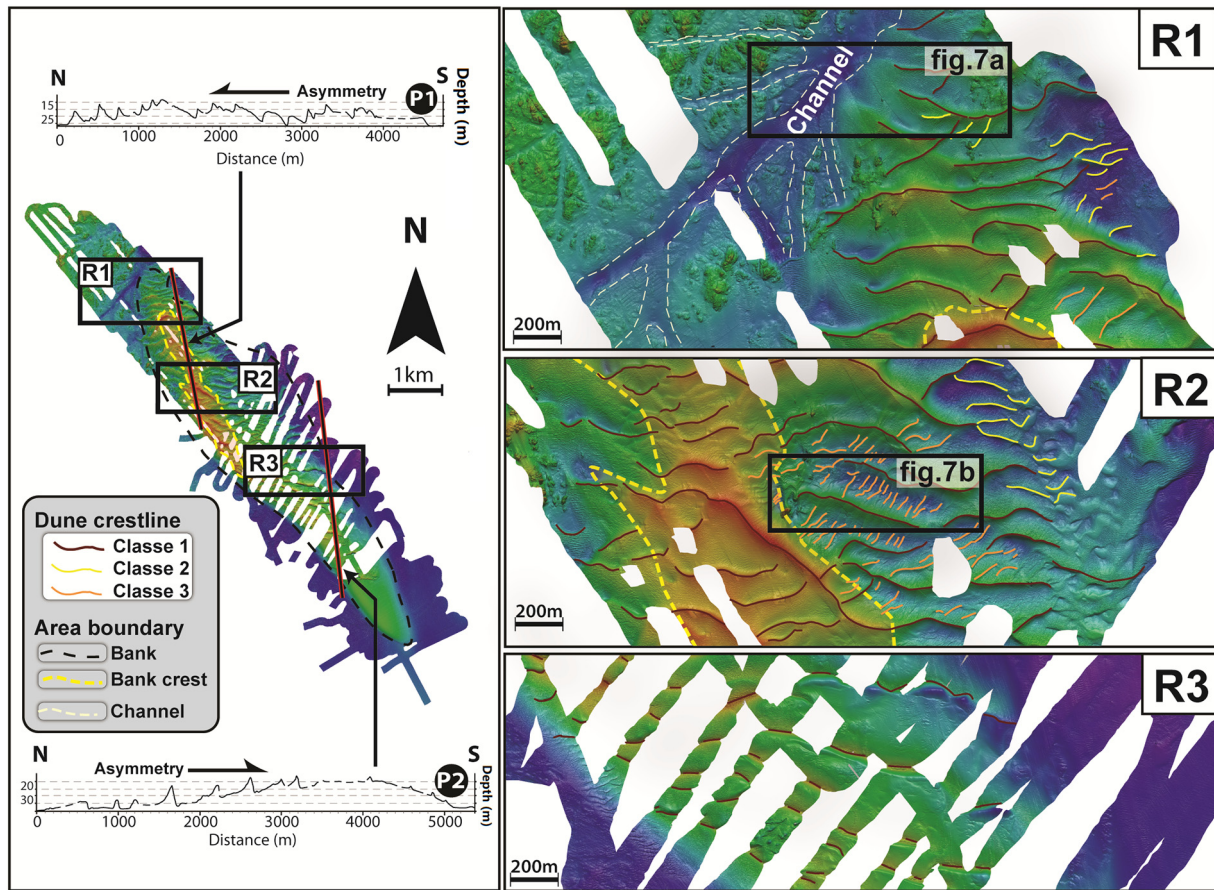


**Fig. 6.** Interpreted bathymetry map of the Horaine Bank; the boxes R1, R2 and R3 correspond to zooms on the different characteristic sectors of the Bank, illustrating the distribution of the main sedimentary bodies associated with the Bank. The class 4 dunes are too small to be illustrated here (see Fig. 7a for more detail).

gentler slope of ca.  $2^\circ$ . The outer envelope of the bank is characterized by a network of dunes of different amplitudes and wavelength that we classified through geostatistical analysis into four main classes according to these parameters (Table 1).

These dune classes are presented below in decreasing order of size and range from very large to small dunes following the classification of Ashley (1990):

**4.1.1. Class 1 – very large dunes:** (Wavelength =  $\sim 215$  m; Height range = 5–11 m)

This class corresponds to the most prominent dunes of the Horaine Bank, characterized by a mean wavelength of 215 m with a height of about 10 m (Table 1, Figs. 6 and 7). With the exception of the distal end of the bank, these dunes are found everywhere with an increasingly marked asymmetry away from the bank crest.

**4.1.2. Class 2 – large- dunes:** (Wavelength =  $\sim 100$  m; Height range = 2–5 m)

These dunes have a wavelength of 100 m and a height of no more than 5 m. They are formed at the extremities of Class 1 dunes and extend as a bifurcation of the latter (Fig. 6R1 and 6R2).

**4.1.3. Class 3 – mid-size-dunes:** (Wavelength =  $\sim 50$  m; Height range = 1–2 m)

These dunes have a 50 m wavelength and a height of around 2 m. They are found in patches separating Class 1 dunes and are oriented perpendicular to them (Figs. 6R2 and Fig. 7). They have a local spatial

extent, being located close to the basal limit of the crest of the bank at depths ranging from 18 m to 28 m (Figs 6R2 and Fig. 7b).

**4.1.4. Class 4 – small-dunes:** (Wavelength  $< 5$  m; Height range  $< 50$  cm)

These are the smallest dunes observable from bathymetric data, with a wavelength shorter than 5 m and a height of less than 50 cm. They develop at the foot of the bank and migrate on the stoss side of class-1 dunes at depths between 20 m and 25 m (Fig. 7a). They are also asymmetrical.

Moreover, for all the asymmetrical dunes of the Horaine Bank, the steeper slopes are seaward on its NW flank and landward on its SE flank (Fig. 6, profiles P1 and P2). As a result, we can unambiguously distinguish two main set of dunes separated by the bank ridge. These two classes seem to exhibit a clockwise rotation around the separation plane (crest of the bank).

## 4.2. Internal structure

The seismic analysis allows us to identify five units (U0 to U4), separated by four bounding surfaces (S1 to S4). Their seismic characteristics are described in Table 2 and each seismic unit is composed of two seismic facies (Fs) for U0, U3 and U4 while U1 and U2 are made up with single seismic facies. We hereafter describe the internal structure of each unit and the morphology of each bounding surface, which are used here to illustrate the morphodynamics of the bedforms associated with the Horaine Bank.



**Table 1**  
List of 50 dunes of the bank randomly selected. The class 4 dunes are too small to be presented here.

| Dunes class | Length (m) | Direction (°) | Max depth (m) | Min depth (m) | Mean depth (m) | Dune height (m) | Lee angle (°) |
|-------------|------------|---------------|---------------|---------------|----------------|-----------------|---------------|
| 1           | 2315.16    | 118           | -21.14        | -8.80         | -14.97         | 9.23            | 19.54         |
| 2           | 199.66     | 89            | -31.27        | -25.53        | -28.40         | 4.35            | 18.79         |
| 2           | 239.97     | 67            | -31.64        | -25.61        | -28.63         | 2.25            | 15.61         |
| 2           | 112.06     | 36            | -28.72        | -24.00        | -26.36         | 3.11            | 12.57         |
| 2           | 189.50     | 83            | -29.24        | -27.73        | -28.49         | 2.48            | 15.41         |
| 1           | 1024.34    | 91            | -25.43        | -15.18        | -20.30         | 7.70            | 22.58         |
| 1           | 1838.37    | 109           | -22.68        | -12.05        | -17.37         | 5.48            | 19.35         |
| 3           | 168.64     | 45            | -25.56        | -16.75        | -21.16         | 1.49            | 13.75         |
| 2           | 214.77     | 80            | -26.90        | -23.71        | -25.30         | 4.08            | 21.75         |
| 1           | 750.39     | 52            | -23.01        | -8.87         | -15.94         | 9.68            | 24.10         |
| 1           | 993.50     | 90            | -20.90        | -12.41        | -16.66         | 9.04            | 12.29         |
| 3           | 127.92     | 51            | -23.72        | -18.70        | -21.21         | 1.80            | 14.66         |
| 3           | 99.52      | 30            | -28.56        | -22.14        | -25.35         | 1.79            | 14.21         |
| 1           | 533.38     | 65            | -22.64        | -9.55         | -16.10         | 5.96            | 21.34         |
| 1           | 381.02     | 89            | -25.37        | -21.55        | -23.46         | 5.53            | 19.60         |
| 1           | 1281.97    | 97            | -20.52        | -8.33         | -14.42         | 7.49            | 13.46         |
| 1           | 890.55     | 90            | -21.74        | -8.04         | -14.89         | 5.36            | 20.19         |
| 3           | 99.90      | 25            | -31.39        | -25.00        | -28.20         | 1.26            | 17.13         |
| 2           | 115.80     | 55            | -22.52        | -18.93        | -20.73         | 3.62            | 10.89         |
| 1           | 1016.26    | 93            | -26.78        | -16.67        | -21.72         | 9.23            | 18.03         |
| 3           | 77.29      | 43            | -27.38        | -22.90        | -25.14         | 1.51            | 15.17         |
| 2           | 425.72     | 75            | -11.11        | -9.79         | -10.45         | 3.73            | 23.10         |
| 3           | 159.33     | 60            | -28.24        | -26.83        | -27.54         | 1.53            | 17.57         |
| 1           | 1053.06    | 83            | -24.06        | -10.49        | -17.28         | 7.70            | 21.19         |
| 3           | 1381.27    | 100           | -20.48        | -14.58        | -17.53         | 1.69            | 6.14          |
| 3           | 50.83      | 47            | -28.69        | -26.48        | -27.59         | 1.05            | 15.66         |
| 3           | 56.12      | 35            | -28.21        | -22.58        | -25.39         | 1.09            | 15.74         |
| 3           | 75.41      | 41            | -29.68        | -22.40        | -26.04         | 1.25            | 15.12         |
| 2           | 221.02     | 82            | -26.98        | -24.94        | -25.96         | 2.24            | 11.33         |
| 2           | 69.04      | 25            | -27.08        | -22.01        | -24.55         | 2.00            | 24.58         |
| 1           | 212.60     | 117           | -28.69        | -14.71        | -21.70         | 6.37            | 16.10         |
| 1           | 410.56     | 68            | -28.43        | -16.02        | -22.22         | 5.90            | 18.33         |
| 2           | 1275.04    | 94            | -32.53        | -14.11        | -23.32         | 4.04            | 24.00         |
| 3           | 106.66     | 53            | -23.89        | -19.82        | -21.85         | 1.52            | 14.11         |
| 2           | 87.51      | 47            | -23.30        | -17.74        | -20.52         | 2.33            | 19.24         |
| 2           | 443.83     | 92            | -25.03        | -18.51        | -21.77         | 4.92            | 18.77         |
| 2           | 125.22     | 28            | -28.46        | -21.94        | -25.20         | 2.16            | 18.22         |
| 1           | 1013.77    | 83            | -26.77        | -17.91        | -22.34         | 7.11            | 15.04         |
| 2           | 196.62     | 109           | -26.96        | -26.81        | -26.89         | 2.24            | 15.38         |
| 3           | 124.21     | 45            | -27.28        | -20.28        | -23.78         | 0.88            | 14.18         |
| 3           | 125.70     | 57            | -28.95        | -27.57        | -28.26         | 1.29            | 13.07         |
| 2           | 151.65     | 89            | -28.38        | -26.25        | -27.32         | 3.15            | 24.74         |
| 2           | 126.91     | 31            | -21.68        | -16.32        | -19.00         | 2.33            | 16.84         |
| 2           | 112.30     | 39            | -22.31        | -20.49        | -21.40         | 3.73            | 14.07         |
| 2           | 294.49     | 102           | -27.10        | -23.80        | -25.45         | 4.32            | 19.75         |
| 1           | 1624.28    | 97            | -24.61        | -11.15        | -17.88         | 8.57            | 19.92         |
| 1           | 588.98     | 83            | -22.74        | -9.57         | -16.15         | 5.07            | 28.72         |
| 1           | 658.16     | 60            | -24.20        | -6.42         | -15.31         | 7.19            | 21.61         |
| 2           | 155.36     | 43            | -26.02        | -19.55        | -22.78         | 2.49            | 21.36         |

#### 4.2.1. Unit U0

Seismic unit U0 is the basal unit of all the seismic profiles analyzed during the survey. It thus extends over the entire Bay of Saint-Brieuc. This unit is bounded at the top by a locally angular irregular surface with monadnocks (Fig. 8b). It is composed of seismic facies Fs1 and Fs2 (Table 2). Facies Fs1 shows chaotic and often diffuse reflections indicative of massive rocks without bedding. Facies Fs2 is characterized by parallel oblique reflectors of low amplitude and medium continuity with an overall sinusoidal configuration of long wavelength (about 400 m). Thus, the U0 unit is interpreted as the Proterozoic basement composed of partially metamorphosed, faulted and deformed igneous and sedimentary rocks forming the bedrock.

#### 4.2.2. Unit U1

Seismic unit U1 corresponds to the basal unit of the Holocene sedimentary filling, it overlies unit U0 with an irregular and truncated surface at the base. It is bounded at the top by a truncated surface. Its acoustic thickness does not exceed 2.5 ms (~4 m) with a local spatial

extent. It is composed exclusively of seismic facies Fs3 with medium-continuous horizontal seismic reflectors of high amplitude. This unit is interpreted as the filling of very small incisions of the bedrock. Due to its basal position, it bears witness to early flooding phases during the Holocene marine transgression.

#### 4.2.3. Unit U2

Seismic unit U2 has a thickness of about 8.5 ms (~14 m), and is only recognized in the hearth of the Horaine Bank (Fig. 8) over an area of 1 km × 7 km. It is bounded at the base by an onlap surface, which overlies unit U0, and locally Unit U1. The top of U2 is overlain by a truncation surface on which the unit U4 rests, and is finally limited laterally by an erosional surface which is overlain by U3. Unit U2 is composed of facies Fs4, which displays a configuration of horizontal and undulating internal reflectors, which then become slightly oblique and prograding at the outer limit of the unit. This unit is interpreted as transgressive deposits sculpted, at the top, by the combined action of tidal currents.

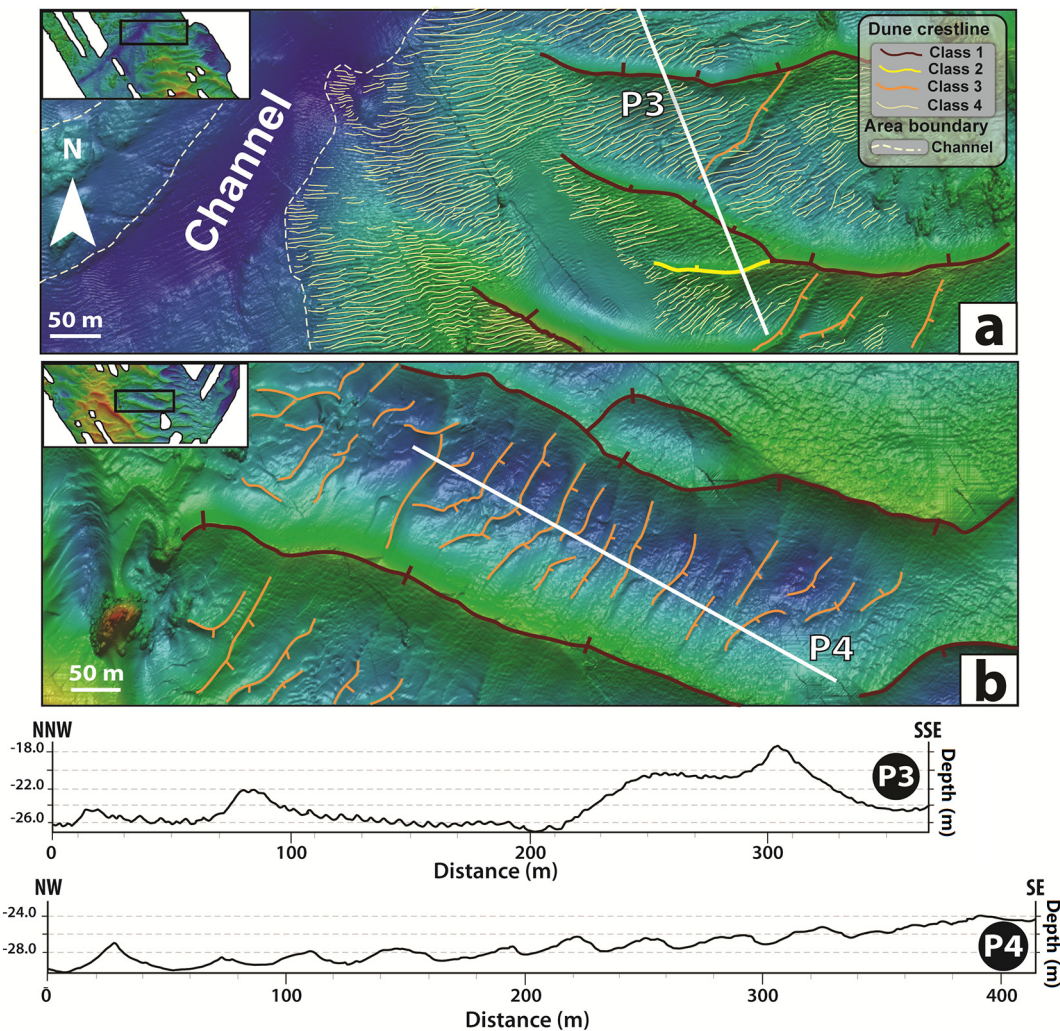


**Fig. 7.** Interpreted bathymetry map of the Horaine Bank; (a) zoom in box R1 of Fig. 6; (b) zoom in box R2 of Fig. 6. (aa) Illustrate the smallest sedimentary bodies (class 4) observable with multibeam echo-sounding.

#### 4.2.4. Unit U3

The U3 unit is recognized in an area extending from the central part of the Horaine Bank to the southwestern extremity (Fig. 8). It is bounded at the base by a downlap.

surface separating it from Unit U0 and at the top by a toplap surface which is overlain by Unit U4 (Fig. 8). However, this latter surface appears truncated at the southwestern end of the bank (Fig. 10e). It is composed of facies Fs5 and Fs6. Facies Fs5 is characterized by moderately continuous seismic reflectors of very low frequency and low amplitudes. It shows an oblique geometric configuration prograding towards the south-western extremity of the bank. Facies Fs6 is characterized by strongly continuous seismic reflectors of medium frequency and low amplitudes.

#### 4.2.5. Unit U4

U4 is the uppermost of the units studied here. It is characterized by seismic facies Fs7 and Fs8. Facies Fs7 shows oblique seismic reflectors prograding onto the Horaine Bank in two fundamentally opposite directions, towards the NE on the NW flank of the bank and towards the SW on the SE flank (Figs. 9 and 10). Facies Fs8 is represented by horizontal to sub-horizontal and locally oblique seismic reflectors prograding in the same way as the dunes migrating towards the head of the bay. This unit thus extends over the entire Bay of Saint-Brieuc and corresponds (i) to the present-day migrating dunes of the upper part of Horaine Bank under the marked influence of tidal currents, and, (ii) to

extensive sandy drapes formed during a sea-level highstand over the entire Bay of Saint-Brieuc.

#### 4.3. Cores

All the vibro-coring data correspond to the seismic unit U4 and indicate a generally homogeneous sedimentary composition according to depth (Fig. 11). However, two groups of cores stand out. The first group (C011, C021 and C022) is located northward of the Bank; it is essentially composed of massive medium to coarse sand (~30%) with shell debris (~70%). This group of cores is also characterized by the presence of a few dark horizons. The second group (C016 and C026) is located southward where we note the presence of coarse sands (~30%) with shell debris (~70%) for the C016 core; and medium sand with an intercalation of very coarse and coarse sand for the C026 core. The latter is also characterized by the presence of dark obliquely stratified horizons.

### 5. Discussion

#### 5.1. Chronostratigraphic setting of the Horaine Bank

Several authors demonstrated that changes in sea level have played an important role in the development of many sandbanks on continental shelves around the world (e.g. Reynaud, 1996; Liu et al., 2007; Liao et al., 2008; Goff, 2014; Zhuo et al., 2014; Flocks et al., 2015; Franzetti

**Table 2**  
Summary of seismic units and these characteristics.

|                    | Unit | Facies | Illustration (Sparker) | Continuity     | Amplitude      | Frequency | Reflectors configuration                    | Interpretation                       | Units configuration |
|--------------------|------|--------|------------------------|----------------|----------------|-----------|---|--------------------------------------|---------------------|
| Sedimentary infill | U4   | Fs8    |                        | Medium to high | Medium to high | High      | Subparallel to parallel                     | sandy drapes                         |                     |
|                    |      | Fs7    |                        | low            | High           | Medium    | oblique prograding or chaotic               | Shell sand dunes                     |                     |
|                    | U3   | Fs6    |                        | Medium         | Medium         | High      | Oblique prograding                          | Gravels and sands of shoreface bars  |                     |
|                    |      | Fs5    |                        | Medium         | Low            | Very low  | Oblique prograding                          | bulk sand deposits                   |                     |
|                    | U2   | Fs4    |                        | High           | High           | Medium    | Subparallel to parallel aggrading           | Estuarine tidal flat sand spit       |                     |
|                    | U1   | Fs3    |                        | Medium         | High           | Medium    | Subparallel to parallel downlap termination | to tidal channels                    |                     |
| Substratum         | U0   | Fs2    |                        | low            | Low            | Medium    | oblique parallel                            | Folded and faulted Sediment basement |                     |
|                    |      | Fs1    |                        | Very Low       | Very low       | Very low  | Chaotic                                     | Cristalline basement                 |                     |

et al., 2015; De Castro et al., 2017). In addition, some authors highlight the role of structural inheritance in the construction and preservation of these continental shelves sedimentary bodies (e.g. Mhammedi, 1994; Bastos et al., 2003; De Castro et al., 2017). Along the Atlantic coast, numerous sandy banks present a sedimentary budget inherited and blocked from the last marine inundation at the foot or proximity of rocky shoals (e.g., Franzetti et al., 2015; Luján et al., 2018; Menier et al., 2016, 2019). The Horaine Bank should be placed in this broadly similar context with a growth stage mostly synchronous to the last sea-level rise and the presence of rocky shoal.

The depositional sequence extracted from the seismic and morphosedimentary study of the Horaine Bank is generally consistent with existing conceptual evolutionary models (Snedden and Dalrymple, 1999; De Castro et al., 2017). Our data provide insights to discuss the role of sea level variations and structural inheritance in the formation and evolution of the Horaine Bank, mainly made up with shell sand and located on the French continental shelf.

With the absence of dated sedimentary infilling of the Bank at depths exceeding 3 m, we conducted radiocarbon dating on the superficial layers by considering a model for the Holocene formation and evolution of the bank, which is based on sea-level curves for the North-West European shelf (Lambeck, 1997, 2004). To be exhaustive, we coupled these later with the model proposed for western Brittany (France) and based on the Sea Level Index Points (SLIP) method (Stéphan and Goslin, 2014).

### 5.2. Structural control and emplacement of seismic unit U1

The Horaine Bank is a N160-trending bedform 12 km long and 2 km wide with an average height of 25 m. It is formed in the lee of a high rocky shoal associated with the Bréhat rocky shoal (Fig. 3b). The N160 elongation direction could be explained by a sedimentary accumulation

constrained by the N160-trending fault system of Nort-sur-Erdre-Quessoy, inherited from the Variscan orogeny in this part of North-Western France and suspected of recent activity during Cenozoic time (Bonnet et al., 2000; Guillocheau et al., 2003) (Fig. 2). In this particular case, we can see a close genetic relationship between a morphological break inherited from the structural history and the localized sedimentary accumulation of the Horaine Bank (Fig. 3b).

The first stages of sea-level rise are characterized by the observation of sedimentary filling within the micro-incisions and the roughness of the Cadomian substratum. This initial filling, defined by seismic unit U1 (Fig. 8e), could correspond to lowstand deposits of fluvial origin reworked during a rise in sea level and accumulated against a linear NNW-SSE trending tectonic structure.

### 5.3. Role of sea-level rise and building up of seismic units U2 and U3

Accelerated sea-level rise during the first stage of the Holocene ~10,000 year BP and 7000 year BP (i.e., up to 13 mm/yr; Lambeck, 1997), led to the rapid flooding of the coastal shelf of the Bay of Saint-Brieuc. This phenomenon along with a significant sedimentary input from the reworking of sediments of the major palaeorivers draining the English Channel (Lericolais et al., 2003; Reynaud et al., 2003), probably led to the building of seismic unit U2. The U2 seismic unit seems to have developed by aggradation in a coastal environment, in a similar way to the sandy spits bordering the current coastlines of the English Channel. The development of a sand spit in the study area took place in a context where rapid rise in sea level was probably the predominant factor in the accumulation of the sedimentary body. The latter is highlighted by our seismic data that show horizontal reflectors and slightly oblique towards the outer limit of the unit U2 (Fig. 8) indicative of a transgressive systems tract. The spit could have continued its development owing to the sedimentary inputs supplied by the longshore

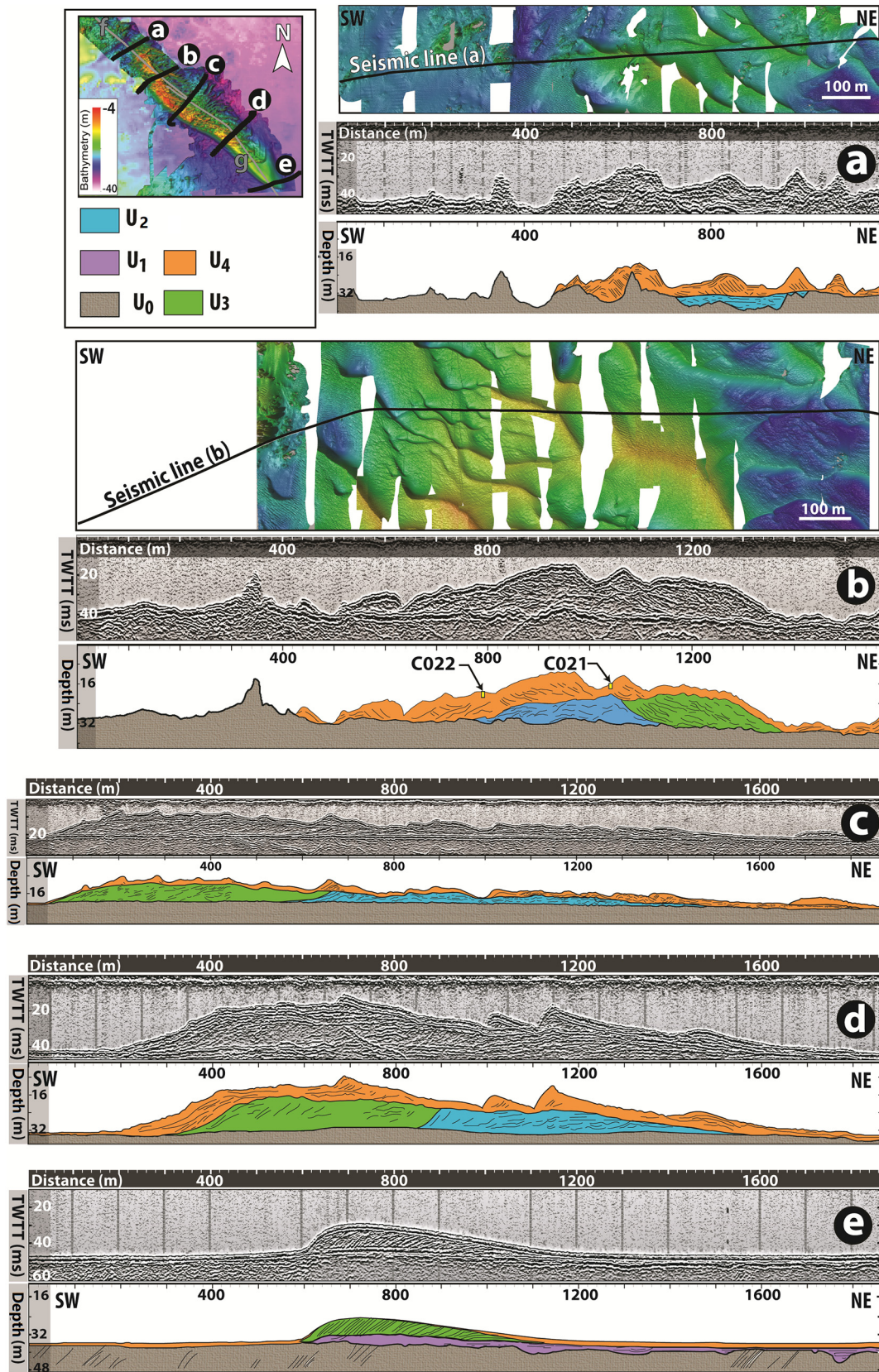
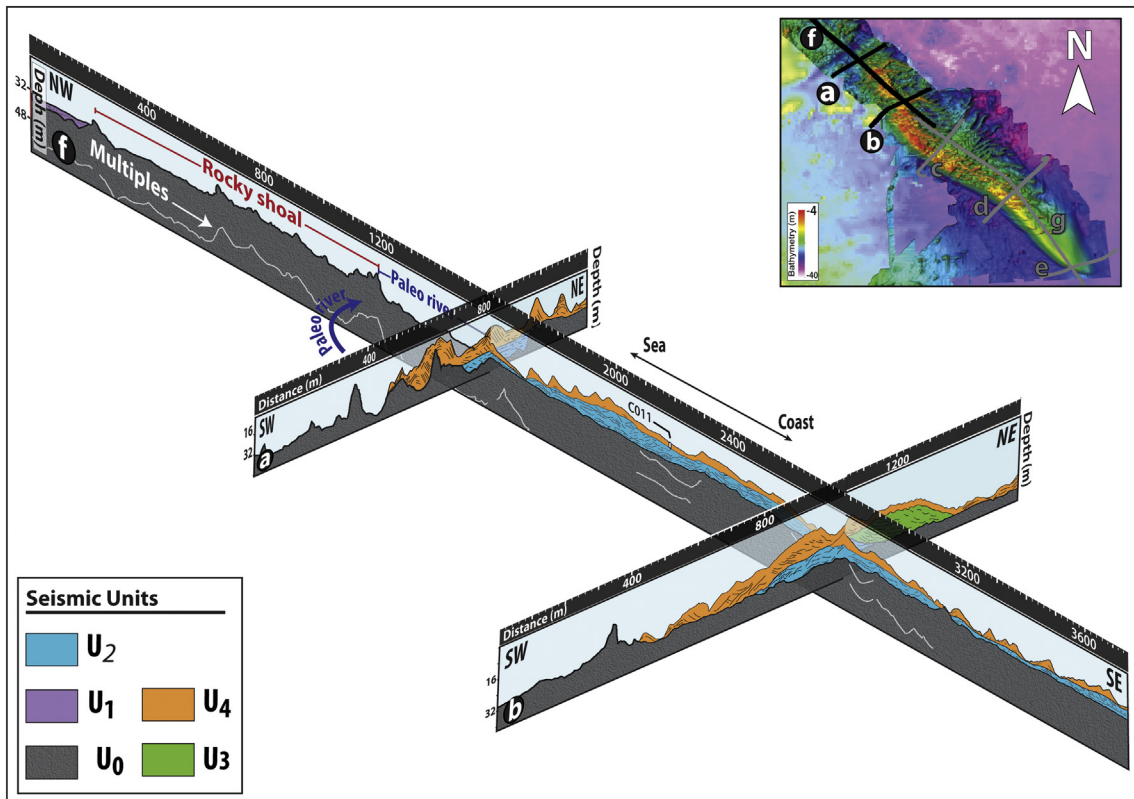


Fig. 8. Seismic profiles used in this study to construct cross-sections of the Horaine Bank. Multibeam echo-sounder bathymetry is presented only for lines a and b; the other lines (c–e) lack usable bathymetric profiles for the illustration. C021 and C022 correspond to cores (see Fig. 11).



**Fig. 9.** 3D representation of selected seismic profiles northwest of the Horaine Bank showing spatial arrangement of the bank in relation to the rocky shoal (f) and the channel separating it from the northern end of the bank, as well as the 3D configuration of seismic reflectors in this area.

drift, controlled by the North-westerly swells which deviate clockwise by the Bréhat plutonic outcrop (Fig. 12, stage 1). In this environment, a back-dune depression is recorded and was subsequently protected by the sand spit, whose floor could have been flooded during

astronomical high tides (as can be observed in the eastern sector of the Bay of Mont Saint Michel (Billeaud, 2007)).

As the marine transgression extended, the flooding of the Horaine spit marks a change in the depositional environment punctuated by:

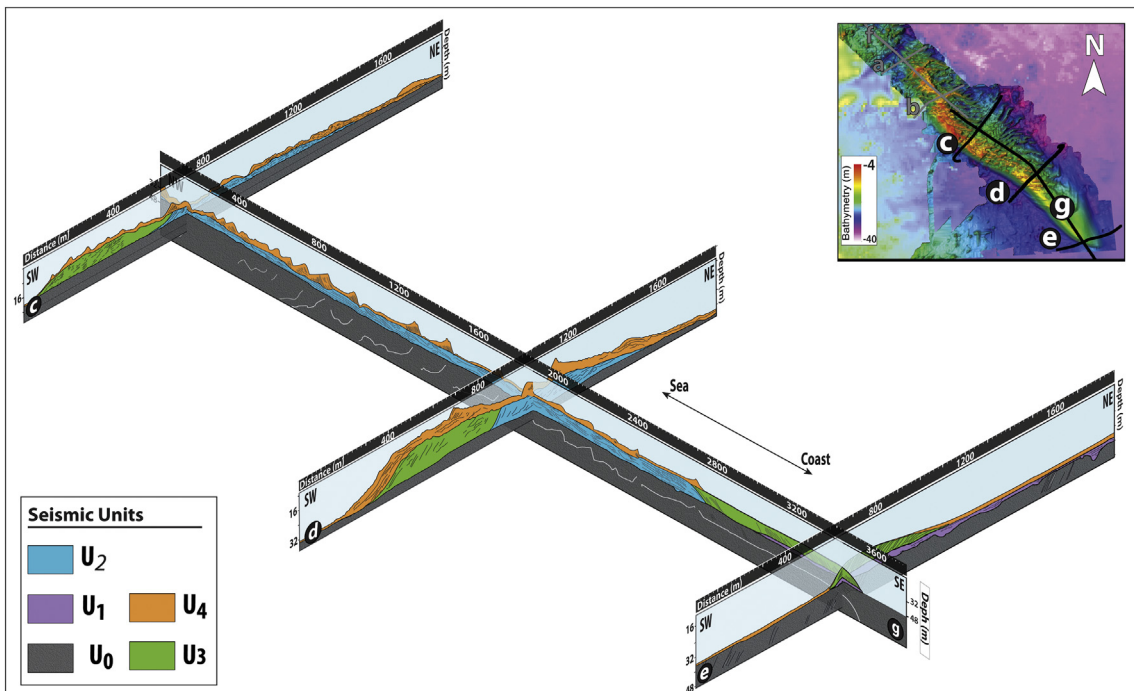


**Fig. 10.** South-easterly continuation of the seismic profiles shown on Fig. 9.

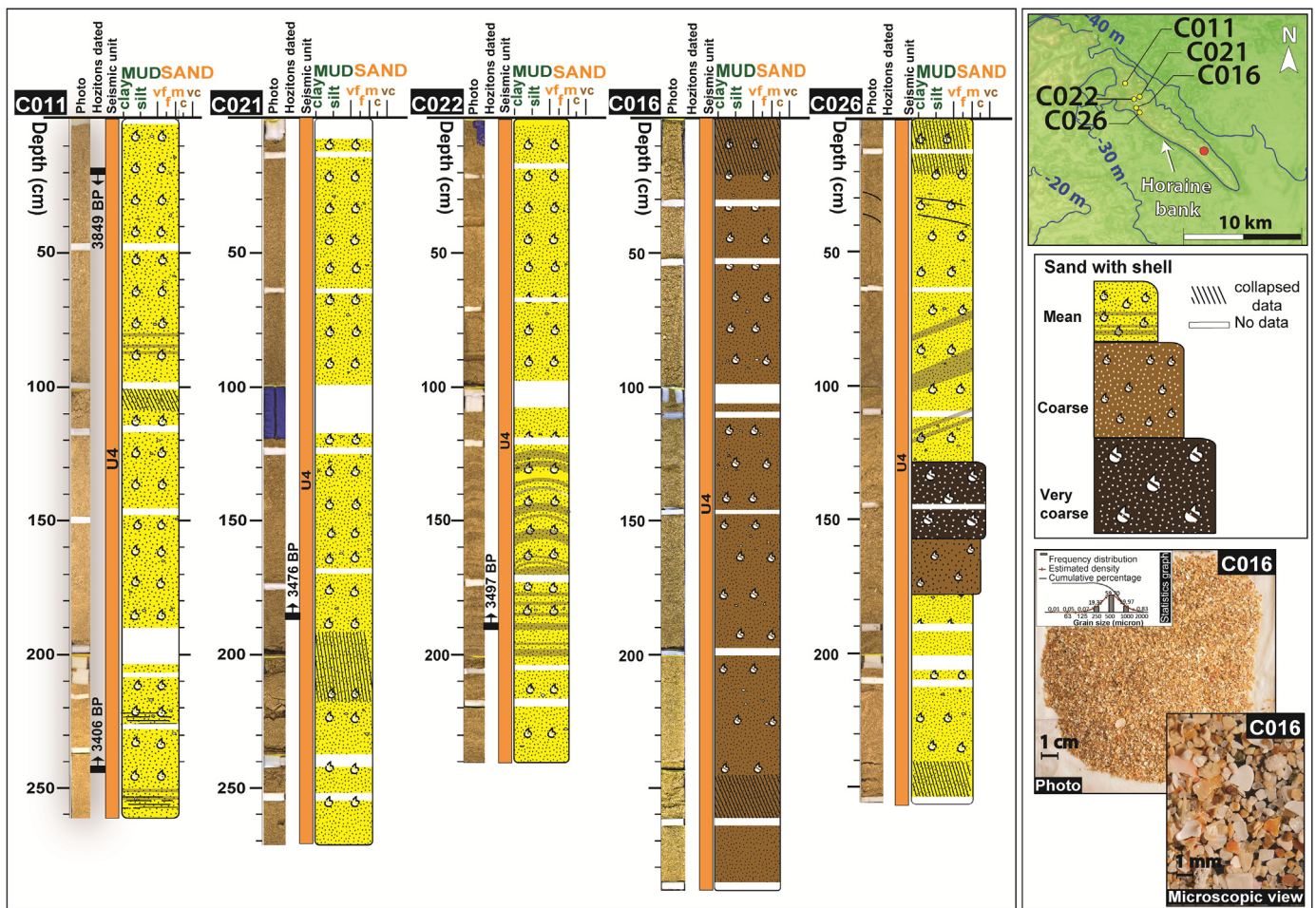


**Fig. 11.** Log description of Cores. Note that horizontal dark lines correspond to the stratification levels. The curved dark horizons in C022 are deformations linked to the stress exerted on the sediments during vibro-core. The shell debris are abundantly occurred in these facies, whose siliciclastic part is dominated by mean to coarse sand. The photos at the bottom right are collected from the top of C016 and allows seeing more lithological details.

(i) erosion of the roof of seismic unit U2, and breaking of the connection between the Bréhat plutonic outcrop and the sandy spit under the probable combined action of tidal currents; (ii) the emplacement of the prograding seismic unit U3 (Fig. 12, stage 2). The deposits associated with unit U3 seem to have accumulated in a short period, with respect to the basal facies Fs5 displaying moderately continuous seismic reflectors with very low frequency and low amplitudes (Table 2). The corresponding basal facies Fs5 could represent sediments derived from the erosion of unit U2 during the flooding phase of the spit. A new physical equilibrium is then established, as indicated by the continuous and regular progradation of unit U3 in a context of rapid transgression (facies Fs6, Table 2).

#### 5.4. Building up of unit 4 and present-day dynamics of the Horaine Bank

The inflection of the sea level rise curve at ~7000 year BP marks the onset of a slowing down of the transgression (i.e., 1.5 mm/yr; (Lambeck, 1997, 2004, Stéphan and Goslin, 2014)). This leads to the build-up of seismic unit U4 corresponding to the migrating dunes superimposed on the Bank. As mentioned above, the U4 corresponding sand dunes seem to rotate clockwise around a separation plane (crestline of the Bank). The strong correlation between the tidal current map (Fig. 5) and the apparent migration directions deduced from morphological analysis of dunes (Fig. 12, present day dynamics), suggest the presence of a tidal gyre controlling the present dynamics of most of the bank

dunes. The orientation of prograding seismic reflectors in unit U4 is consistent with the present-day direction of dune migration, indicating that tidal control was continuously maintained until present-day. This last hypothesis is corroborated by the ~3500 year BP radiocarbon-dated age of the U4 samples (Table 3).

The sediment composition of these dunes is comparable to other known banks (Berné et al., 1994; De Castro et al., 2017) with the presence of numerous debris of bivalve and gastropod shells (~70%) for all the cores taken from unit U4 (Fig. 11). These shells, dated at ~3500 year BP, are contemporary with major upheavals observed in the coastal sedimentary systems of the Channel-Atlantic (Long and Hughes, 1995; Billeaud et al., 2009; Tessier et al., 2012; Van Vliet-Lanoë et al., 2014a, 2014b). These upheavals are characterized by an increase in precipitation and storminess (Geel et al., 1996; Clarke and Rendell, 2009). In this specific case, we can envisage that these shell debris are the result of a remobilization of bivalves and gastropods of low and medium foreshore occupying the near-shore environment of the coasts of West Brittany and are trapped today behind the Bréhat rocky shoal due to the presence of a tidal gyre.

Analysis of the U4 seismic unit, which forms a drape over the entire Bay of Saint-Brieuc, reveals that the sedimentary thickness is greater in the western sector than in the east. The western sector is thus characterized by the presence of the Horaine Bank and a set of dunes migrating towards the south, at the head of the bay. The asymmetrical distribution of the bayhead dunes between the east and west of the bay implies that

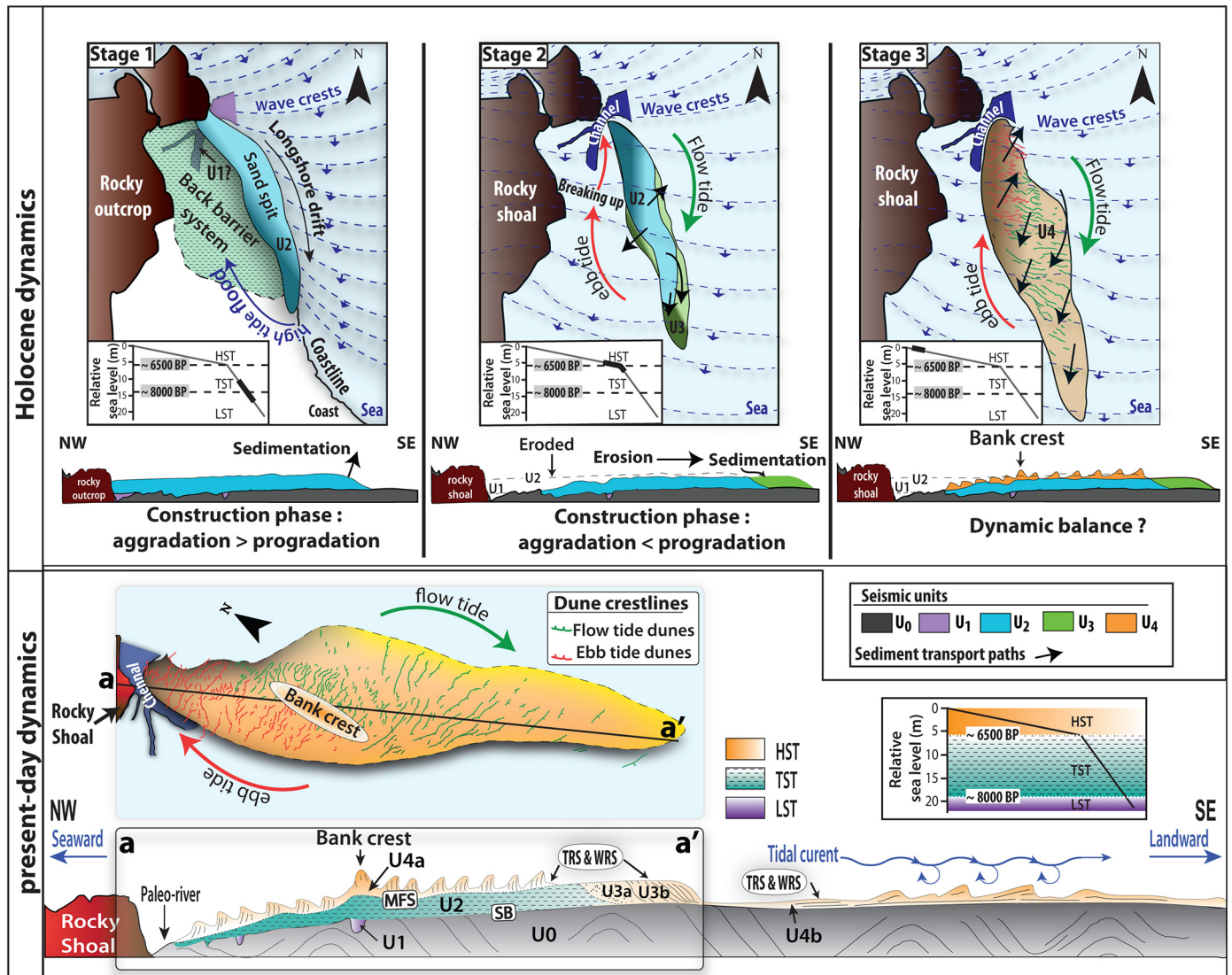


Fig. 12. Synthetic conceptual model of the Horaine Bank dynamics. At top, model of the bank construction on a Holocene scale. At bottom, present-day dynamics of the bank illustrating its role in the sediment supply of adjacent coastlines; the tide current dunes have been digitalized from bathymetry data.

**Table 3**  
Marker horizons dated through AMS radiocarbon dating on samples of shell sand (see Fig. 11).

| Sample name    | Lab. code   | Depth (cm) | Material   | Age <sup>14</sup> C (yr) | Error | Age Cal. yr BP |            |
|----------------|-------------|------------|------------|--------------------------|-------|----------------|------------|
|                |             |            |            |                          |       | min            | max (mean) |
| C11_1 3-0.23   | Poz-130,181 | 25         | Shell sand | 3820                     | 30    | 3616–4083      | (3849)     |
| C11_3 3-W-0.36 | Poz-130,182 | 240        | Shell sand | 3465                     | 30    | 3193–3619      | (3406)     |
| C21_2 3-0.85   | Poz-130,183 | 185        | Shell sand | 3525                     | 30    | 3263–3690      | (3476)     |
| C22_2 3-0.9    | Poz-130,184 | 190        | Shell sand | 3540                     | 30    | 3283–3712      | (3497)     |

these dunes originate from the Horaine Bank and migrate to supply sediments towards the bay head (Fig. 12, present-day dynamics), where there is a significant infilling.

In view of its morphosedimentary configuration, the Bay of Saint-Brieuc is located on one of the major sediment transit paths distributed over the whole of the North-Western European shelf (Stride, 1963).

### 6. Conclusion

The seabed of the Bay of Saint-Brieuc is covered by a formation made up of sandy, silico-clastic and carbonate deposits with an average

thickness of about 10 m and locally reaching up to 25 m. This formation is thickest in the NW sector of the bay and corresponds to the inherited and composite Horaine Bank emplaced during the last marine flooding. Sequence stratigraphic analysis of the sedimentary geometry, based on very high-resolution seismic profile data, shows that the formation consists of a single depositional sequence corresponding to the last Quaternary glacio-eustatic cycle between isotope stages 3 and 1. The base of the sequence is marked by a phase of erosion of the substratum (U0), corresponding to periods of emergence over the entire of the bay, when sediments in transit away from the present-day coastline were captured by the major paleorivers of the Channel. The glacio-eustatic

rise in sea level, along with the structural inheritance allowed the sedimentary filling of very small incisions and the emplacement of a seismic unit (U1) probably with very heterogeneous lithology that could be of fluvial-estuarine and/or colluvial origin (head flow/solifluction). Above this basal U1 unit, transgressive parasequences are deposited and, correspond to seismic unit U2. This unit seems to have developed, by longshore drift, in a context where rapid rise in sea level was probably the predominant factor in the sedimentary deposits. The marine flooding of unit U2 is followed by the emplacement of the U3 seismic unit, showing a configuration of reflectors prograding towards the coast and, forced by tidal currents and storm swells. The unit U3 is overlain by Unit 4, whose geometry and extent indicate a continuation of the previous hydrodynamic conditions but under decreasing water column depth due to accommodation. This unit extends over entire of the Bay of Saint-Brieuc and corresponds (i) to the present-day migrating dunes of the upper part of Horaine Bank and, (ii) to extensive sandy drapes formed during a sea-level highstand over the entire Bay of Saint-Brieuc. Longitudinal dunes on the eastern flank of the Bank of the Horaine display an asymmetry, which indicates their migration towards the coast. On the western flank of the bank, we observe an inversion of the migration around a nodal point located approximately in the sector of the Horaine Bank crest. Unit U4 is seen to be migrating, with changes in its sedimentary thickness and volume; some of the sediment remains in a stationary dynamic, while another part is lost, giving rise to bedforms migrating towards the south of the Bay of Saint-Brieuc. This may be the main source of the sediment supply towards the coast, where there is significant beach nourishment. In perspective, our research is set to discuss and quantify volumes and evidences of significant cross-shore migration from offshore to onshore, along the littoral region, and continue to investigate with high resolution the evolution of sandy beaches and their findings to the offshore sedimentary budget.

### Declaration of Competing Interest

The authors declare that they have no known competing financial interests or personal relationships that could have appeared to influence the work reported in this paper.

### Acknowledgement

Many thanks to University of South Brittany, France for funding this study. We would like to thank the crews of the R/V “Côtes de la Manche”. We thank also Delphine Pierre, Charline Guérin and Laure Simplet, geophysical engineers at IFREMER, for their assistance in processing the bathymetric data. Many thanks to the “Compagnie Armoricaïne de Navigation (CAN)” especially to Anais Guérin.

### References

Ashley, G.M., 1990. Classification of large-scale subaqueous bedforms; a new look at an old problem. *J. Sediment. Res.* 60, 160–172. <https://doi.org/10.2110/jsr.60.160>.

Augris, C., Chantal, S.B., Garreau, P., Guenoc, P., Guénolé, A., Hamon, D., Houlgate, E., 1996. Atlas thématique de l'environnement marin en baie de Saint-Brieuc (Côtes-d'Armor). IFREMER, pp. 1–76 (in French).

Auvray, B., Charlot, R., Vidal, P., 1980. Données nouvelles sur le Protérozoïque inférieur du domaine nord-Armoricain (France): âge et signification. *Can. J. Earth Sci.* 17, 532–538 (in French).

Ballèvre, M., Bosse, V., Dabard, M.-P., Ducassou, C., Fourcade, S., Paquette, J.-L., Peucat, J.-J., Pitra, P., 2013. Histoire géologique du Massif armoricain: actualité de la recherche. *Bull. Soc. Géol. Minéral. Bretagne* 500, 5–96 (in French).

Bastos, A.C., Collins, M., Kenyon, N.H., 2003. Morphology and internal structure of sand shoals and sandbanks off the Dorset coast, English Channel. *Sedimentology* 50, 1105–1122. <https://doi.org/10.1046/j.1365-3091.2003.00596.x>.

Berné, S., 1999. Dynamique, architecture et préservation des corps sableux de plate-forme. HDR, pp. 1–118 (in French).

Berné, S., Trentesaux, A., Stolk, A., Missiaen, T., de Batist, M., 1994. Architecture and long term evolution of a tidal sandbank: the Middelkerke Bank (southern North Sea). *Mar. Geol.* 121, 57–72. [https://doi.org/10.1016/0025-3227\(94\)90156-2](https://doi.org/10.1016/0025-3227(94)90156-2).

Bessin, P., 2014. Evolution géomorphologique du Massif Armoricaïn depuis 200 Ma: approche Terre-Mer. Ph.D. thesis. Rennes 1 University, pp. 1–377 (in French).

Billeaud, I., 2007. Dynamique de construction d'un prisme sédimentaire littoral en régime mégatidal (la Baie du Mont-Saint-Michel). Ph. D thesis. Université Caen Normandie, pp. 1–239 (in French).

Billeaud, I., Tessier, B., Lesueur, P., 2009. Impacts of late Holocene rapid climate changes as recorded in a macrotidal coastal setting (Mont-Saint-Michel Bay, France). *Geology* 37, 1031–1034. <https://doi.org/10.1130/G30310A.1>.

Bitri, A., Brun, J.P., Truffert, C., Guennoc, P., 2001. Deep seismic imaging of the Cadomian thrust wedge of Northern Brittany. *Tectonophysics* 331, 65–80. [https://doi.org/10.1016/S0040-1951\(00\)00236-5](https://doi.org/10.1016/S0040-1951(00)00236-5).

Bois, C., Cazes, M., Gariel, O., Lefort, J.-P., Le Gall, B., 1991. Principaux apports scientifiques des campagnes SWAT et WAM à la géologie de la mer Celtique, de la Manche et de la marge Atlantique. *Mém. Soc. Géol. Fr.* 1833 (159), 185–217 (In French).

Bonnet, S., Guillocheau, F., Brun, J.-P., Van Den Driessche, J., 2000. Large-scale relief development related to Quaternary tectonic uplift of a Proterozoic-Paleozoic basement: the Armorican Massif, NW France. *J. Geophys. Res. Solid Earth* 105, 19273–19288.

Caston, V.N.D., Stride, A.H., 1970. Tidal sand movement between some linear sand banks in the North Sea off Northeast Norfolk. *Mar. Geol.* 9, M38–M42. [https://doi.org/10.1016/0025-3227\(70\)90018-6](https://doi.org/10.1016/0025-3227(70)90018-6).

Chantraine, J., Egal, E., Thiéblemont, D., Le Goff, E., Guerrot, C., Ballèvre, M., Guennoc, P., 2001. The Cadomian active margin (North Armorican Massif, France): a segment of the North Atlantic Panafrikan belt. *Tectonophysics* 331, 1–18. [https://doi.org/10.1016/S0040-1951\(00\)00233-X](https://doi.org/10.1016/S0040-1951(00)00233-X).

Chantraine, J., Autran, A., Cavalier, C., 2003. Carte géologique de la France à 1/1 000 000 6ème édition révisée. Orléans BRGM (In French).

Chaumillon, E., Bertin, X., Falchetto, H., Allard, J., Weber, N., Walker, P., Pouvreau, N., Woppelmann, G., 2008. Multi time-scale evolution of a wide estuary linear sandbank, the Longe de Boyard, on the French Atlantic coast. *Mar. Geol.* 251, 209–223. <https://doi.org/10.1016/j.margeo.2008.02.014>.

Chaumillon, E., Tessier, B., Reynaud, J.-Y., 2010. Stratigraphic records and variability of incised valleys and estuaries along French coasts. *Bull. Soc. Géol. Fr.* 181, 75–85. <https://doi.org/10.2113/gssgfbull.181.2.75>.

Clarke, M.L., Rendell, H.M., 2009. The impact of North Atlantic storminess on western European coasts: a review. *Quat. Int. Hurricanes Typhoons: Field Rec. Forecast* 195, 31–41. <https://doi.org/10.1016/j.quaint.2008.02.007>.

De Castro, S., Lobo, F.J., 2018. Sedimentary infilling of bedrock-controlled palaeo-embayments off Cape Trafalgar, Strait of Gibraltar (Gulf of Cadiz). *Geo-Mar. Lett.* 38, 47–62. <https://doi.org/10.1007/s00367-017-0508-4>.

De Castro, S., Lobo, F.J., Puga-Bernabéu, Á., 2017. Headland-associated banner banks generated during the last deglaciation near the Strait of Gibraltar (Gulf of Cadiz, SW Spain). *Mar. Geol.* 386, 56–75. <https://doi.org/10.1016/j.margeo.2017.02.007>.

Del Estal, N., Mathew, M.J., Menier, D., Gensac, E., Delanoë, H., Le Gall, R., Joostens, T., Rouille, A., Guillemet, B., Lemaitre, G., 2019. Chapter 11 - An assessment of the administrative-legal, physical-natural, and socio-economic subsystems of the Bay of Saint Brieuc, France: Implications for effective coastal zone management. In: Ramkumar, Mu, James, R.A., Menier, D., Kumaraswamy, K. (Eds.), *Coastal Zone Management*. Elsevier, pp. 251–276. <https://doi.org/10.1016/B978-0-12-814350-6.00011-2>.

Flocks, J.G., Kindinger, J.L., Kelso, K.W., 2015. Geologic control on the evolution of the inner shelf morphology offshore of the Mississippi barrier islands, northern Gulf of Mexico, USA. *Cont. Shelf Res.* 101, 59–70. <https://doi.org/10.1016/j.csr.2015.04.008>.

Franzetti, M., Le Roy, P., Delacourt, C., Garlan, T., Cancouët, R., Sukhovich, A., Deschamps, A., 2013. Giant dune morphologies and dynamics in a deep continental shelf environment: example of the banc du four (Western Brittany, France). *Mar. Geol.* 346, 17–30. <https://doi.org/10.1016/j.margeo.2013.07.014>.

Franzetti, M., Le Roy, P., Garlan, T., Graindorge, D., Sukhovich, A., Delacourt, C., Le Dantec, N., 2015. Long term evolution and internal architecture of a high-energy banner ridge from seismic survey of Banc du four (Western Brittany, France). *Mar. Geol.* 369, 196–211. <https://doi.org/10.1016/j.margeo.2015.08.019>.

Geel, B.V., Buurman, J., Waterbolk, H.T., 1996. Archaeological and palaeoecological indications of an abrupt climate change in the Netherlands, and evidence for climatological teleconnections around 2650 BP. *J. Quat. Sci.* 11, 451–460. [https://doi.org/10.1002/\(SICI\)1099-1417\(199611/12\)11:6<451::AID-JQS275>3.0.CO;2-9](https://doi.org/10.1002/(SICI)1099-1417(199611/12)11:6<451::AID-JQS275>3.0.CO;2-9).

Goff, J.A., 2014. Seismic and core investigation off Panama city, Florida, reveals sand ridge influence on formation of the shoreface ravinement. *Cont. Shelf Res.* 88, 34–46. <https://doi.org/10.1016/j.csr.2014.07.006>.

Graviou, P., 1992. Reconnaissance d'une suture majeure au sein de la chaîne cadomienne. *Comptes Rendus Académie Sci. Sér. 2 Mécanique. Phys. Chim. Sci. Univers Sci. Terre* 315, 1799–1802 (in French).

Gregoire, G., Le Roy, P., Ehrhold, A., Jouet, G., Garlan, T., 2017. Control factors of Holocene sedimentary infilling in a semi-closed tidal estuarine-like system: the bay of Brest (France). *Mar. Geol.* 385, 84–100. <https://doi.org/10.1016/j.margeo.2016.11.005>.

Guilcher, A., 1950. L'île de Béniguet (Finistère), exemple d'accumulation en queue de comète. *Bull. Inf. Com. Cent. Océan. Etude Côtes II* 7, 243–250 (in French).

Guillocheau, F., Brault, Thomas, Barbarand, J., Bonnet, S., Bourquin, S.J.E.-C., Guennoc, P., Menier, D., Néraudeau, D., Proust, J.-N., Wyns, R., 2003. Histoire géologique du Massif Armoricaïn depuis 140 Ma (Crétacé-Actuel). *Assoc. Géol. Bassin Paris* 40, 13–28 (in French).

Heaton, T.J., Köhler, P., Butzin, M., Bard, E., Reimer, R.W., Austin, W.E.N., Ramsey, C.B., Grootes, P.M., Hughen, K.A., Kromer, B., Reimer, P.J., Adkins, J., Burke, A., Cook, M.S., Olsen, J., Skinner, L.C., 2020. Marine20—the marine radiocarbon age calibration curve (0–55,000 cal BP). *Radiocarbon* 62, 779–820. <https://doi.org/10.1017/RDC.2020.68>.

Houbolt, J., 1968. Recent sediments in the southern bight of the North Sea. *Geol. En Mijnb.* 47, 245–273.



- Hulscher, S.J.M.H., De Swart, H.E., De Vriend, H.J., 1993. The generation of offshore tidal sand banks and sand waves. *Cont. Shelf Res.* 13, 1183–1204. [https://doi.org/10.1016/0278-4343\(93\)90048-3](https://doi.org/10.1016/0278-4343(93)90048-3).
- Huthnance, J.M., 1982. On one mechanism forming linear sand banks. *Estuar. Coast. Shelf Sci.* 14, 79–99. [https://doi.org/10.1016/S0302-3524\(82\)80068-6](https://doi.org/10.1016/S0302-3524(82)80068-6).
- Lambeck, K., 1997. Sea-level change along the French Atlantic and Channel coasts since the time of the last Glacial Maximum. *Palaeogeogr. Palaeoclimatol. Palaeoecol.* 129, 1–22. [https://doi.org/10.1016/S0031-0182\(96\)00061-2](https://doi.org/10.1016/S0031-0182(96)00061-2).
- Lambeck, K., 2004. Sea-level change through the last glacial cycle: geophysical, glaciological and palaeogeographic consequences. *Compt. Rendus Geosci.* 336, 677–689. <https://doi.org/10.1016/j.crte.2003.12.017>.
- Larsonneur, C., Auffret, J.-P., Caline, B., Gruet, Y., Lautridou, J.-P., 1994. The Bay of Mont-Saint-Michel: a sedimentation model in a temperate macrotidal environment. *Senckenberg. Maritima Frankfurt/Main* 24, 3–63.
- Lericolais, G., Auffret, J.-P., Bourillet, J.-F., 2003. The Quaternary channel river: seismic stratigraphy of its palaeo-valleys and deeps. *J. Quat. Sci.* 18, 245–260. <https://doi.org/10.1002/jqs.759>.
- Liao, H.-R., Yu, H.-S., Su, C.-C., 2008. Morphology and sedimentation of sand bodies in the tidal shelf sea of eastern Taiwan Strait. *Mar. Geol.* 248, 161–178. <https://doi.org/10.1016/j.margeo.2007.10.013>.
- Liu, Z., Berné, S., Saito, Y., Yu, H., Trentesaux, A., Uehara, K., Yin, P., Paul Liu, J., Li, C., Hu, G., Wang, X., 2007. Internal architecture and mobility of tidal sand ridges in the East China Sea. *Cont. Shelf Res.* 27, 1820–1834. <https://doi.org/10.1016/j.csr.2007.03.002>.
- Long, A.J., Hughes, P.D.M., 1995. Mid- and late-Holocene evolution of the Dungeness foreland, UK. *Mar. Geol.* 124 (1), 253–271. [https://doi.org/10.1016/0025-3227\(95\)00044-Y](https://doi.org/10.1016/0025-3227(95)00044-Y).
- Luján, M., Lobo, F.J., Bruno, M., de Castro, S., 2018. Morpho-stratigraphic features of the northern shelf of the Strait of Gibraltar: Tectonic and sedimentary processes acting at different temporal scales. *Cont. Shelf Res.* 162, 13–26. <https://doi.org/10.1016/j.csr.2018.04.005>.
- Marsset, T., Tessier, B., Reynaud, J.-Y., De Batist, M., Plagnol, C., 1999. The Celtic Sea banks: an example of sand body analysis from very high-resolution seismic data. *Mar. Geol.* 158, 89–109. [https://doi.org/10.1016/S0025-3227\(98\)00188-1](https://doi.org/10.1016/S0025-3227(98)00188-1).
- Mathew, M.J., Sautter, B., Ariffin, E.H., Menier, D., Ramkumar, M., Siddiqui, N.A., Delanoe, H., Del Estal, N., Traoré, K., Gensac, E., 2020. Total vulnerability of the littoral zone to climate change-driven natural hazards in North Brittany, France. *Sci. Total Environ.* 706, 135963. <https://doi.org/10.1016/j.scitotenv.2019.135963>.
- Menier, D., 2018. GEOSAINTEBRIEUC18 Cruise, Thalia R/V. <https://doi.org/10.17600/18000412>.
- Menier, D., Reynaud, J.-Y., Proust, J.-N., Guillocheau, F., Guennoc, P., Bonnet, S., Tessier, B., Goubert, E., 2006. Basement Control on Shaping and Infilling of Valleys Incised at the Southern Coast of Brittany, France. *S.E.P.M. Soc. Sedimen. Geol. Spec. Publ.* 85, 37–55. <https://doi.org/10.2110/pec.06.85.0037>.
- Menier, D., Tessier, B., Proust, J.N., Baltzer, A., Sorrel, P., Traini, C., 2010. The Holocene transgression as recorded by incised-valley infilling in a rocky coast context with low sediment supply (southern Brittany, western France). *Bull. Soc. Geol. Fr.* 181, 115–128. <https://doi.org/10.2113/gssgfbull.181.2.115>.
- Menier, D., Estournès, G., Mathew, M.J., Ramkumar, M., Briand, C., Siddiqui, N., Traini, C., Pian, S., Labeyrie, L., 2016. Relict geomorphological and structural control on the coastal sediment partitioning, North of Bay of Biscay. *Z. Für. Geomorphol.* 60, 67–74.
- Menier, D., Mathew, M., Cherfils, J.-B., Ramkumar, M., Estournès, G., Koch, M., Guillocheau, F., Sedrati, M., Goubert, E., Gensac, E., Le Gall, R., Novico, F., 2019. Holocene Sediment Mobilization in the Inner Continental Shelf of the Bay of Biscay: implications for regional sediment budget offshore to onshore. *J. Coast. Res.* 88, 110–121. <https://doi.org/10.2112/S188-009.1>.
- Mhammedi, N., 1994. Architecture du banc sableux tidal de Sercq (Iles Anglo-Normandes). Ph.D thesis. Université des sciences et technologies de Lille, pp. 1–215 (in French).
- Poncellet, C., Billant, G., Corre, M.-P., 2020. Globe (Global Oceanographic Bathymetry Explorer) Software. SEANOE <https://doi.org/10.17882/70460>.
- Quesney, A., 1983. Manche occidentale et Mer Celtique: étude des paléovallées, des fosses et des formations surperçielles. Ph.D thesis. Université de Caen, pp. 1–162 (in French).
- Reynaud, J.-Y., 1996. Ph.D thesis. Architecture et évolution d'un banc sableux de mer celtique méridionale. Université des sciences et technologies de Lille, pp. 1–196 (in French).
- Reynaud, J.-Y., Tessier, B., Proust, J.-N., Dalrymple, R., Marsset, T., Batist, M.D., Bourillet, J.-F., Lericolais, G., 1999. Eustatic and hydrodynamic controls on the architecture of a deep shelf sand bank (Celtic Sea). *Sedimentology* 46, 703–721. <https://doi.org/10.1046/j.1365-3091.1999.00244.x>.
- Reynaud, J.-Y., Tessier, B., Auffret, J.-P., Berné, S., Batist, M.D., Marsset, T., Walker, P., 2003. The offshore Quaternary sediment bodies of the English Channel and its Western Approaches. *J. Quat. Sci.* 18, 361–371. <https://doi.org/10.1002/jqs.758>.
- S.H.O.M., 1968. Courants de marée dans la Manche et sur les côtes françaises de l'Atlantique. Imprimerie Nationale, Paris, pp. 1–287 (in French).
- Snedden, J., Dalrymple, R., 1999. Modern shelf sand ridges: From historical perspective to a unified hydrodynamic and evolutionary model. In: Bergman, K.M., Snedden, J.W. (Eds.), *Isolated Shallow Marine Sand Bodies: Sequence Stratigraphic Analysis and Sedimentologic Interpretation*. SEPM Society for Sedimentary Geology, pp. 13–28.
- Sorrel, P., Tessier, B., Demory, F., Delsinne, N., Mouzè, D., 2009. Evidence for millennial-scale climatic events in the sedimentary infilling of a macrotidal estuarine system, the Seine estuary (NW France). *Quat. Sci. Rev.* 28, 499–516. <https://doi.org/10.1016/j.quascirev.2008.11.009>.
- Stéphan, P., Goslin, J., 2014. Évolution du niveau marin relatif à l'Holocène le long des côtes françaises de l'Atlantique et de la Manche: réactualisation des données par la méthode des "sea-level index points". *Quaternaire* 25, 295–312 (In French). <https://doi.org/10.4000/quaternaire.7269>.
- Stride, A.H., 1963. Current-swept Sea floors near the southern half of Great Britain. *Q. J. Geol. Soc.* 119, 175–197. <https://doi.org/10.1144/gsjgs.119.1.0175>.
- Swift, D.J.P., Thorne, J.A., 1991. Sedimentation on continental margins, I: A general model for shelf sedimentation. In: Swift, D.J.P., Oertel, G.F., Tillman, R.W., Thorne, J.A. (Eds.), *Shelf Sand and Sandstone Bodies: Geometry, Facies and Sequence Stratigraphy*. The International Association of Sedimentologists, pp. 1–31.
- Tessier, B., Delsinne, N., Sorrel, P., 2010. Holocene sedimentary infilling of a tide-dominated estuarine mouth. The example of the macrotidal Seine estuary (NW France). *Bull. Soc. Géol. Fr.* 181, 87–98. <https://doi.org/10.2113/gssgfbull.181.2.87>.
- Tessier, B., Billeaud, I., Sorrel, P., Delsinne, N., Lesueur, P., 2012. Infilling stratigraphy of macrotidal tide-dominated estuaries. Controlling mechanisms: Sea-level fluctuations, bedrock morphology, sediment supply and climate changes (the examples of the Seine estuary and the Mont-Saint-Michel Bay, English Channel, NW France). *Sediment. Geol.* 279, 62–73. <https://doi.org/10.1016/j.sedgeo.2011.02.003>.
- Tisnérat-Laborde, N., Paterne, M., Métivier, B., Arnold, M., Yiou, P., Blamart, D., Reynaud, S., 2010. Variability of the Northeast Atlantic Sea surface  $\Delta 14C$  and marine reservoir age and the North Atlantic Oscillation (NAO). *Quat. Sci. Rev.* 29, 2633–2646. <https://doi.org/10.1016/j.quascirev.2010.06.013>.
- Trentesaux, A., Stolk, A., Berné, S., 1999. Sedimentology and stratigraphy of a tidal sand bank in the southern North Sea. *Mar. Geol.* 159, 253–272. [https://doi.org/10.1016/S0025-3227\(99\)00007-9](https://doi.org/10.1016/S0025-3227(99)00007-9).
- Van Vliet-Lanoë, B., Goslin, J., Hallégouët, B., Hénaff, A., Delacourt, C., Fernane, A., Franzetti, M., Le Cornec, E., Le Roy, P., Penaud, A., 2014a. Middle- to late-Holocene storminess in Brittany (NW France): part I – morphological impact and stratigraphical record. *The Holocene* 24, 413–433. <https://doi.org/10.1177/0959683613519687>.
- Van Vliet-Lanoë, B., Penaud, A., Hénaff, A., Delacourt, C., Fernane, A., Goslin, J., Hallégouët, B., Le Cornec, E., 2014b. Middle- to late-Holocene storminess in Brittany (NW France): Part II – the chronology of events and climate forcing. *The Holocene* 24, 434–453. <https://doi.org/10.1177/0959683613519688>.
- Walker, P., 2001. Dynamique sédimentaire dans le golfe normand-breton: intérêt de l'imagerie par sonar à balayage latéral. Ph.D thesis. Université Caen Normandie, pp. 1–289 (in French).
- Wang, Y., Liu, Y., Jin, S., Sun, C., Wei, X., 2019. Evolution of the topography of tidal flats and sandbanks along the Jiangsu coast from 1973 to 2016 observed from satellites. *ISPRS J. Photogramm. Remote Sens.* 150, 27–43. <https://doi.org/10.1016/j.isprsjprs.2019.02.001>.
- Zhuo, H., Wang, Y., Shi, H., Zhu, M., He, M., Chen, W., Li, H., 2014. Seismic geomorphology, architecture and genesis of Miocene shelf sand ridges in the Pearl River Mouth Basin, northern South China Sea. *Mar. Pet. Geol.* 54, 106–122. <https://doi.org/10.1016/j.marpetgeo.2014.03.002>.